NASA TN D-1033

NASA TN D-1033

IN-06
390137

NASA

TECHNICAL NOTE

D-1033

STATIC STABILITY AND CONTROL OF CANARD CONFIGURATIONS

AT MACH NUMBERS FROM 0.70 TO 2.22 - TRIANGULAR

WING AND CANARD WITH TWIN VERTICAL TAILS

By Victor L. Peterson

Ames Research Center
Moffett Field, Calif.

NATIONAL AERONAUTICS AND SPACE ADMINISTRATION

WASHINGTON   June 1961

NATIONAL AERONAUTICS AND SPACE ADMINISTRATION

TECHNICAL NOTE D-1033

STATIC STABILITY AND CONTROL OF CANARD CONFIGURATIONS

AT MACH NUMBERS FROM 0.70 TO 2.22 - TRIANGULAR

WING AND CANARD WITH TWIN VERTICAL TAILS

By Victor L. Peterson

SUMMARY

The static aerodynamic characteristics of a canard airplane configuration having twin vertical stabilizing surfaces are presented. The model consisted of a wing and canard both of triangular plan form and aspect ratio 2 mounted on a Sears-Haack body of fineness ratio 12.5 and two swept and tapered wing-mounted vertical tails of aspect ratio 1.35. Data are presented for Mach numbers from 0.70 to 2.22 and for angles of attack from $-6°$ to $+18°$ at $0°$ and $5°$ sideslip. Tests were made with the canard off and with the canard on. Nominal canard deflection angles ranged from $0°$ to $10°$. The Reynolds number was 3.68×10^6 based on the wing mean aerodynamic chord.

Selected portions of the data obtained in this investigation are compared with previously published results for the same model having a single vertical tail instead of twin vertical tails. Without the canard, the directional stability at supersonic Mach numbers and high angles of attack was improved slightly by replacing the single tail with twin tails. However, at a Mach number of 0.70, the directional stability of the twin-tail model deteriorated rapidly with increasing angle of attack above $10°$ and fell considerably below the level for the single-tail model. At subsonic speeds the directional stability of the twin-tail model with the canard was comparable to that for the single-tail model and at supersonic speed it was considerably greater at high angles of attack. Unlike the single-tail model, the twin-tail model at $5°$ sideslip exhibited an unstable break in the variation of pitching-moment coefficient with lift coefficient near $10°$ angle of attack for 0.70 Mach number.

INTRODUCTION

The possible gains to be realized at supersonic speeds in the form of reduced trim drag and increased maneuverability by the use of canards rather than conventional tail-aft controls have resulted in considerable interest in these arrangements. Therefore, an extensive experimental program aimed at determining the static longitudinal, lateral, and

directional characteristics of a number of canard airplane configurations was undertaken by the NASA Research Centers. Results of previous investigations in this program, such as those reported in reference 1, have demonstrated the reduction in trim drag of canard configurations at supersonic speeds as compared to trailing-edge-flap and aft-mounted horizontal tail arrangements. However, it has also been shown (ref. 1) that the use of canards can result in either beneficial or detrimental interference effects on directional stability at high angles of attack, depending on the vertical-tail arrangement.

The purpose of the present investigation was to provide experimental information on the static aerodynamic characteristics of a canard configuration having twin vertical tails and to compare the results with those reported in references 2 and 3 for a similar canard configuration with a single vertical tail. The twin-tail and single-tail models differed only in the number and placement of the vertical stabilizing surfaces. The results of an earlier investigation in which the pressure distributions on the twin-tail canard configuration were measured have been reported in reference 4. Results of other phases of recent NASA canard research are presented in references 5 through 11.

The present investigation was conducted in the Ames 6- by 6-Foot Supersonic Wind Tunnel and covered a Mach range from 0.70 to 2.22 with angles of attack to 18° with 0° and 5° of sideslip. Nominal canard deflection angles ranged from 0° to 10°. The Reynolds number was 3.58×10^6 based on the wing mean aerodynamic chord.

<div align="right">A 5 0 8</div>

NOTATION

b	wing span
$\bar{c}$	mean aerodynamic chord of wing
C_D	drag coefficient, $\dfrac{\text{drag}}{qS}$
C_{D_o}	drag coefficient at zero lift
C_L	lift coefficient, $\dfrac{\text{lift}}{qS}$
C_{L_α}	lift-curve slope taken through zero angle of attack, per deg
C_m	pitching-moment coefficient, $\dfrac{\text{pitching moment}}{qS\bar{c}}$, referred to projection of the $0.21\bar{c}$ point on the body center line
C_l	rolling-moment coefficient, $\dfrac{\text{rolling moment}}{qSb}$

C_n yawing-moment coefficient, $\dfrac{\text{yawing moment}}{qSb}$, referred to the projection of the $0.21\bar{c}$ point on the body center line

C_Y side-force coefficient, $\dfrac{\text{side force}}{qS}$

$\dfrac{\Delta C_l}{\beta}$ difference between rolling-moment coefficients at $5°$ and $0°$ sideslip divided by $5°$, per deg

$\dfrac{\Delta C_n}{\beta}$ difference between yawing-moment coefficients at $5°$ and $0°$ sideslip divided by $5°$, per deg

$\dfrac{\Delta C_Y}{\beta}$ difference between side-force coefficients at $5°$ and $0°$ sideslip divided by $5°$, per deg

l length of body before truncation

$\left(\dfrac{L}{D}\right)_{max}$ maximum lift-drag ratio

M free-stream Mach number

q free-stream dynamic pressure

r local body radius

r_0 maximum body radius

S wing plan-form area including the area formed by extending the leading and trailing edges to the plane of symmetry

x distance aft of body nose

α angle of attack of wing root chord, deg

β sideslip angle between the relative wind and the vertical plane of symmetry, deg

δ angle of deflection of the canard with respect to the wing chord plane, positive when trailing edge is down, deg

MODEL AND APPARATUS

The model consisted of a triangular wing and an all-movable triangular canard, each having an aspect ratio of 2.0, swept and tapered vertical tails of aspect ratio 1.35, and a Sears-Haack body of fineness ratio 12.5. Photographs of the model without and with the canard are presented in figures 1(a) and 1(b), respectively. A dimensional sketch

of the complete model is presented in figure 1(c) and the canard is detailed in figure 1(d). The wing and vertical tails had NACA 0003-63 sections streamwise, and the canard consisted of a flat plate with beveled leading and trailing edges. The canard hinge line, passing through the 0.35 point of its mean aerodynamic chord, was located in the extended wing chord plane 1.21 wing mean aerodynamic chord lengths ahead of the reference center of moments. The ratio of the exposed area of the canard to the total area of the wing was 6.9 percent and the ratio of the total areas was 12.9 percent. The twin vertical tails were mounted on the wing panels at mid-semispan. The plan form, aspect ratio, and combined plan-form area of the twin tails were identical to those for the single vertical tail of references 2 and 3. All other components of the present configuration were identical to those of references 2 and 3. For convenience, a sketch of the model with the single tail used in the studies reported in references 2 and 3 is shown in figure 1(e).

The model was sting-mounted in the wind tunnel. An internal, six-component, strain-gage balance measured the forces and moments on the entire configuration.

TESTS AND PROCEDURES

Ranges of Test Variables

Mach numbers of 0.70, 1.30, 1.70, and 2.22, and angles of attack from -6° to +18° with 0° and 5° sideslip were covered in the investigation. Nominal canard deflection angles ranged from 0° to 10°. The test Reynolds number based on the wing mean aerodynamic chord was 3.68×10^6. To induce boundary-layer transition at fixed locations on the model, wires of 0.010-inch diameter were placed on both surfaces of the wing and wires of 0.005-inch diameter were affixed to all surfaces of the canard and vertical tails at the locations shown in figure 1(c). For tests of the model with no canard, a 0.010-inch-diameter transition wire was located on the body 4 inches from the nose. Although there were no measurements of the increment of the form drag coefficient contributed by the transition wires, previous studies have indicated this increment to be less than 0.0010. All the data presented herein are for transition-fixed conditions.

Reduction of Data

The data presented herein have been reduced to standard coefficient form. Rolling-moment, side-force, yawing-moment, and pitching-moment coefficients were referred to the body axes. Lift and drag coefficients were referred to the wind axes. The pitching-moment and yawing-moment coefficients were referred to the projection on the body center line of

the 0.21 point of the wing mean aerodynamic chord. This particular moment-center location was chosen so that the data would be consistent with those for the single-tail configuration reported in references 2 and 3.

The base pressure was measured and the data were adjusted to correspond to a base pressure equal to the free-stream static pressure. The data were also adjusted for stream inclinations in the model pitch plane which were less than $\pm0.3^\circ$ at all Mach numbers. No corrections to model sideslip angle were applied for wind-tunnel stream angularities in the lateral plane. A survey of the wind-tunnel stream made subsequent to the test of the model showed the stream angularities in the lateral plane to be of the order of 0.25° at $M = 0.70$, and $M = 1.30$ and zero at $M = 2.22$.

RESULTS AND DISCUSSION

Lateral and Directional Characteristics

Effects of the canard.- The rolling-moment, side-force, and yawing-moment coefficients (C_l, C_Y, C_n) for the twin-tail model with and without the canard are presented in figure 2 as a function of angle of attack for sideslip angles of 0° and 5°. At zero sideslip these coefficients have values near zero for all test variables. The slight deviations from zero are a result of the combined effects of model asymmetry, wind-tunnel-stream irregularities, and the inaccuracy of measurements.

For a sideslip angle of 5° the data show that the canard surface generally produced only small effects on the side-force coefficients while some rather large effects on the yawing-moment and rolling-moment coefficients were incurred. For all test Mach numbers, the yawing-moment coefficients for the model at 5° of sideslip were increased considerably at moderate to high angles of attack by the addition of the canard surface. At supersonic speeds for 5° of sideslip, the addition of the canard surface generally increased the magnitude of the rolling-moment coefficients over the entire range of positive angles of attack. Similar increases in rolling moments were evident for a Mach number of 0.70 at the lower angles of attack; however, at higher angles of attack $(\alpha > 14^\circ)$ the effect of the canard on the rolling moment was reversed.

Comparisons of single- and twin-tail characteristics with the canard off.- Comparisons of the incremental parameters $\Delta C_l/\beta$, $\Delta C_Y/\beta$, and $\Delta C_n/\beta$ for twin- and single-tail models without a canard are made in figure 3. The results for twin tails were obtained from figure 2 and the results for a single tail from reference 3. Below an angle of attack of about 10°, the single vertical tail produced more side force for all test Mach numbers than did the twin vertical tails. The

opposite might have been expected on the basis of exposed vertical surface area. The twin tails extended behind the trailing edge of the wing, however, and possibly had a lower effective aspect ratio as a result of reduced end-plate effect. Other influencing factors are the relative positions of the tails and the sidewash fields due to the body and wing vortices, and possibly mutual interference between the twin tails. As angle of attack was increased above $10°$ for supersonic speeds, the twin tails eventually produced more side force than the single tail. This situation did not exist for a Mach number of 0.70; in fact, the side-force derivative for the twin-tail model decreased rapidly with increasing angle of attack above $10°$.

The differences between the directional stability parameter $\Delta C_n/\beta$ for the two models follow the same general trends with angle of attack and Mach number as the side-force derivatives. Thus, for supersonic speeds the twin-tail model had less stability than the single-tail model at low angles of attack and slightly more stability at high angles of attack. For a Mach number of 0.70 the single-tail model did not experience the rapid deterioration of directional stability with increasing angle of attack above $10°$ measured for the twin-tail model. (In comparing values of $\Delta C_n/\beta$ it should be noted that the single tail had a slightly longer yawing-moment arm than did the twin tails.) The differences in the effective dihedral $\Delta C_l/\beta$ for the two models at any of the test conditions probably would not have significant effects on over-all aerodynamic performance.

The results in figure 3 have shown that for the model without the canard, nothing was gained from the standpoint of improving directional stability by replacing the single vertical tail with the twin tails for the arrangements tested. The slight improvement in directional stability with twin tails noted for supersonic Mach numbers and high angles of attack was more than offset by the unfavorable angle-of-attack effects on the directional stability for a Mach number of 0.70.

Comparisons of single- and twin-tail characteristics with the canard on.- Comparisons of the incremental parameters $\Delta C_l/\beta$, $\Delta C_Y/\beta$, and $\Delta C_n/\beta$ for twin- and single-tail models with a canard are made in figure 4. The results for twin tails were obtained from figure 2 and the results for a single tail from reference 3. The results in figure 4 show that the effects of vertical-tail position on the side-force derivatives were similar in one respect to the effects measured for the models without the canard; that is, the side-force derivatives were smaller in magnitude for the twin-tail model at low angles of attack for all test Mach numbers. As angle of attack was increased at supersonic speeds, the side-force derivatives for the single-tail model decreased while those for the twin-tail model remained almost constant. Thus, for supersonic speeds, the twin tails produced considerably more side force at high angles of attack than did the single tail. For a Mach number of 0.70, however, both tail arrangements produced about the same amount of side force.

Comparisons of the directional stability parameter $\Delta C_n/\beta$ at supersonic speeds show that the twin-tail model maintained significantly higher directional stability at high angles of attack than the single-tail model. Deflection of the canard affected the directional stability of both models favorably at angles of attack above about 10°. For a Mach number of 0.70, both models retained a high level of directional stability for angles of attack up to the limit of the tests.

For a Mach number of 0.70 (fig. 4(a)) the single-tail model did not experience the abrupt reduction in $\Delta C_l/\beta$ between 10° and 14° angle of attack measured for the twin-tail model. It may be concluded that the primary cause of the deterioration of effective dihedral for the twin-tail model is interference between the loadings on the twin vertical tails and the wing since the variations of the side-force derivatives are nearly the same for the two models. Measured loadings on the wings of the single- and twin-tail models are presented in reference 4. Comparison of these data shows that the addition of twin tails did, in fact, reduce the loading on the windward wing panel at $M = 0.70$, $\beta = 5.3°$ and $\alpha > 8°$ when the canard was either on or off, with the largest reductions measured for the canard on. No wing loading data are available for the leeward wing panels of these models.

The results in figure 4 have shown that for the model with the canard the use of twin vertical tails instead of a single vertical surface can improve directional stability at high angles of attack and supersonic Mach numbers. Furthermore, in contract to the results for the model without the canard, the twin-tail configuration maintained adequate directional stability at $M = 0.70$. The rather abrupt nonlinearities in the variation of the effective dihedral $\Delta C_l/\beta$ with angles of attack might prove to be a problem with the use of twin tails although positive dihedral effect was maintained throughout the angle-of-attack range investigated.

Longitudinal Characteristics

The lift, drag, and pitching-moment coefficients for the twin-tail model with and without the canard are presented in figure 5 for zero sideslip. Some of the results of figure 5 are summarized as a function of Mach number in figure 6 and compared with those for the single-tail model from reference 3. The results in figure 6(a) for the model without the canard show that the aerodynamic-center locations, zero-lift drag coefficients, and lift-curve slopes were not significantly different for the two tail arrangements at supersonic speeds. For a Mach number of 0.70, the only important difference is in the maximum lift-drag ratio which was larger for the twin-tail model. Nearly all this difference was due to a difference in the drag due to lift since the minimum drag coefficients are about the same for the two models. Similar differences for the two tail arrangements were obtained for the model with the canard (fig. 6(b)).

The lift, drag, and pitching-moment coefficients for the twin-tail model with and without the canard are presented in figure 7 for a side-slip angle of 5°. The results in figure 7(a) for a Mach number of 0.70 show a rather abrupt unstable tendency in the variation of pitching-moment coefficient with lift coefficient at an angle of attack of about 10°. This marked change in stability was not evident at any of the supersonic Mach numbers investigated.

In the previous discussion of lateral and directional character-istics, it was pointed out that the nonlinearities of the effective dihedral parameter $\Delta C_l/\beta$ with respect to angle of attack at $M = 0.70$ were believed to be a result of effects on the wing caused by interfer-ence from the twin vertical tails. If this were the case, differences between the longitudinal characteristics of the twin- and single-tail models would also be expected with the models in sideslip. The lift and pitching-moment coefficients for the two models with and without the canard at 5° sideslip are compared in figure 8 at one subsonic and one supersonic Mach number. The pitching-moment results for a Mach number of 0.70 (fig. 8(a)) are quite different for the two models. These data show that the unstable break in the variation of pitching-moment coeffi-cient with lift coefficient noted in the above discussion is caused by the twin tails. In addition, the data for a Mach number of 0.70 (fig. 8(b)) show that the twin tails caused a reduction of lift above about 10° angle of attack. Because the reduction of lift-curve slope occurs in the same angle-of-attack range as the pitch-up tendency, the majority of the loss in lift must result from reduced lift aft of the reference center of moments. The pressure-distribution results in refer-ence 4 substantiate this finding. The comparisons of the data shown in figure 8 for $M = 1.70$ are typical of all supersonic Mach numbers investigated. They show that the lift and pitching-moment characteristics of the models with the two tail arrangements are not significantly different in this Mach number range.

CONCLUSIONS

The static aerodynamic characteristics of an airplane model with twin vertical stabilizing surfaces with and without a canard surface were measured. Comparisons of these data with those for a model iden-tical except for a single vertical surface revealed the following:

1. Without a canard surface the directional stability at super-sonic Mach numbers and high angles of attack was improved slightly by replacing the single vertical tail with twin tails. For a Mach number of 0.70, the directional stability with twin tails deteriorated rapidly with increasing angle of attack above 10°, while that for a single tail remained relatively constant.

2. With the canard surface the use of twin tails instead of the single tail resulted in significant increases in directional stability at supersonic Mach numbers and high angles of attack without the large unfavorable effect on the directional stability evident for a Mach number of 0.70 without the canard.

3. The model with twin tails exhibited an unstable break in the variation of pitching-moment coefficient with lift coefficient at an angle of attack of about 10° at 5° sideslip for a Mach number of 0.70. For the same test conditions, the effective dihedral $\Delta C_l/\beta$ was nonlinear with respect to angle of attack.

A
5
0
8

Ames Research Center
      National Aeronautics and Space Administration
            Moffett Field, Calif., April 18, 1961

<div align="center">REFERENCES</div>

1. Hall, Charles F., and Boyd, John W.: Effects of Canards on Airplane Performance and Stability. NACA RM A58D24, 1958.

2. Boyd, John W., and Peterson, Victor L.: Static Stability and Control of Canard Configurations at Mach Numbers From 0.70 to 2.22 - Longitudinal Characteristics of a Triangular Wing and Canard. NACA RM A57J15, 1958.

3. Peterson, Victor L., and Menees, Gene P.: Static Stability and Control of Canard Configurations at Mach Numbers From 0.70 to 2.22 - Lateral-Directional Characteristics of a Triangular Wing and Canard. NACA RM A57L18, 1958.

4. Peterson, Victor L., and Menees, Gene P.: Aerodynamic Loads at Mach Numbers From 0.70 to 2.22 on an Airplane Model Having a Wing and Canard of Triangular Plan Form and Either Single or Twin Vertical Tails. NASA TN D-690, 1961.

5. Boyd, John W., and Peterson, Victor L.: Static Stability and Control of Canard Configurations at Mach Numbers From 0.70 to 2.22 - Triangular Wing and Canard on an Extended Body. NACA RM A57K14, 1958.

6. Peterson, Victor L., and Menees, Gene P.: Static Stability and Control of Canard Configurations at Mach Numbers From 0.70 to 2.22 - Longitudinal Characteristics of a Triangular Wing and Unswept Canard. NACA RM A57K26, 1958.

7. Hedstrom, C. Ernest, Blackaby, James R., and Peterson, Victor L.: Static Stability and Control Characteristics of a Triangular Wing and Canard Configuration at Mach Numbers From 2.58 to 3.53. NACA RM A58C05, 1958.

8. Buell, Donald A., and Tinling, Bruce E.: The Static Longitudinal Stability and Control Characteristics in the Presence of the Ground of a Model Having a Triangular Wing and Canard. NASA MEMO 3-4-59A, 1959.

9. Peterson, Victor L.: Static Stability and Control of Canard Configurations at Mach Numbers From 0.70 to 2.22 - Lateral-Directional Characteristics of an Unswept Wing and Canard. NASA MEMO 4-20-59A, 1959.

10. Boyd, John W., and Menees, Gene P.: Longitudinal Stability and Control Characteristics at Mach Numbers From 0.70 to 2.22 of a Triangular Wing Configuration Equipped with a Canard Control, a Trailing-Edge-Flap Control, and a Cambered Forebody. NASA MEMO 4-21-59A, 1959.

11. Driver, Cornelius, and Jacocks, James L.: Tabulated Data From a Pressure-Distribution Investigation at Mach Number 2.01 of the Wing of a Canard Airplane Model. NASA TM X-140, 1959.

A
5
0
8

A-26079

(a) Photograph of model without canard.

A-25916

(b) Photograph of model with canard.

Figure 1.- Model details and dimensions.

0.010 diam.
transition wire

Center of moments, 0.21 $\bar{c}$

$\bar{c}$ = 17.64

r_o = 2.38

63°26'

12.54

26.46

15.85

0.005 diam.
transition wire

Hinge line

7.00

All dimensions in inches

13.22

6.99

26.46

0.005 diam.
transition wire

2.22

3.50

56°30'

7.83

8.08

36.12

46.90

r

x

Equation of body ordinates:

$$\frac{r}{r_o} = \left[1 - \left(1 - \frac{2x}{l} \right)^2 \right]^{\frac{3}{4}}$$
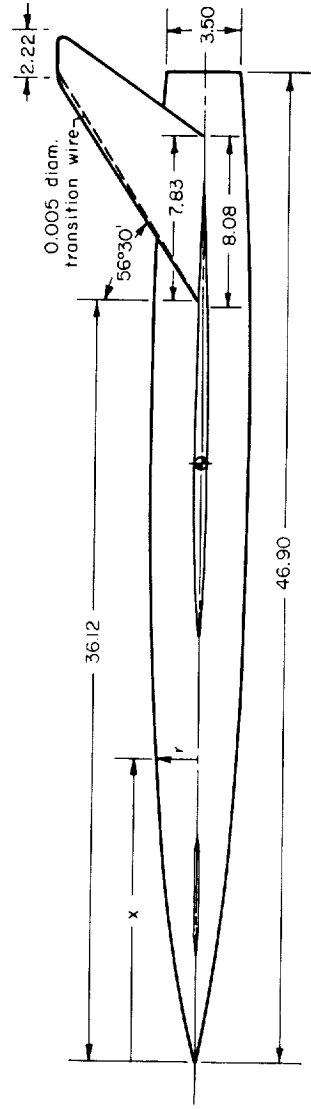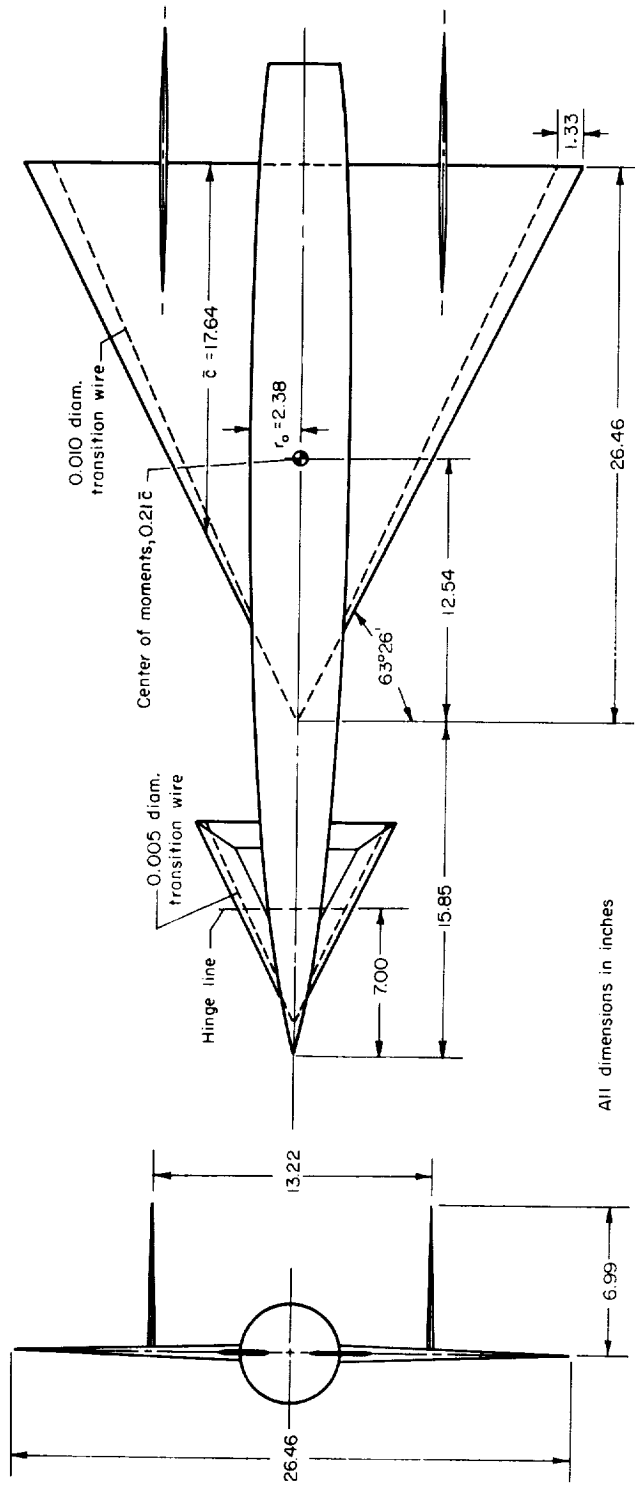
l = theoretical body length = 59.50

(c) Dimensional sketch of twin-tail model.

Figure 1.- Continued.

A
5
0
8

9.50

8.00

4.12

1.00

Hinge line

1.20

9.50

63°26'

Canard-body gap
at δ = 0 is 0.020

All dimensions in inches

A

A

0.20

Section A-A

5°7'

9°30'
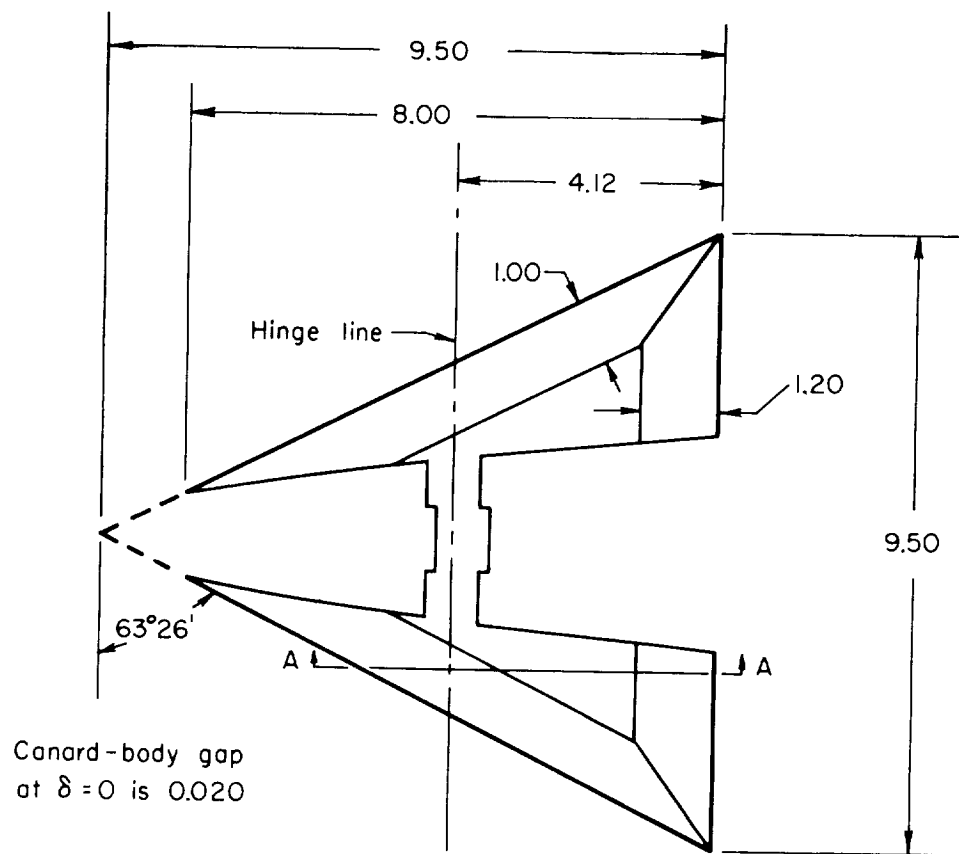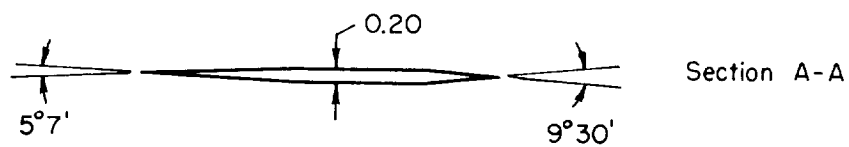
(d) Details of canard surface.

Figure 1.- Continued.

0.010 diam.
transition wire

Center of moments, 0.210

0.005 diam.
transition wire

Hinge line

$\bar{c}=17.64$

$r_0=2.38$

$63°26'$

1.33

26.46

12.54

15.85

7.00

26.46

9.90

All dimensions in inches

3.14

3.50

0.005 diam.
transition wire

$56°30'$

11.43

46.90

36.25

r

x
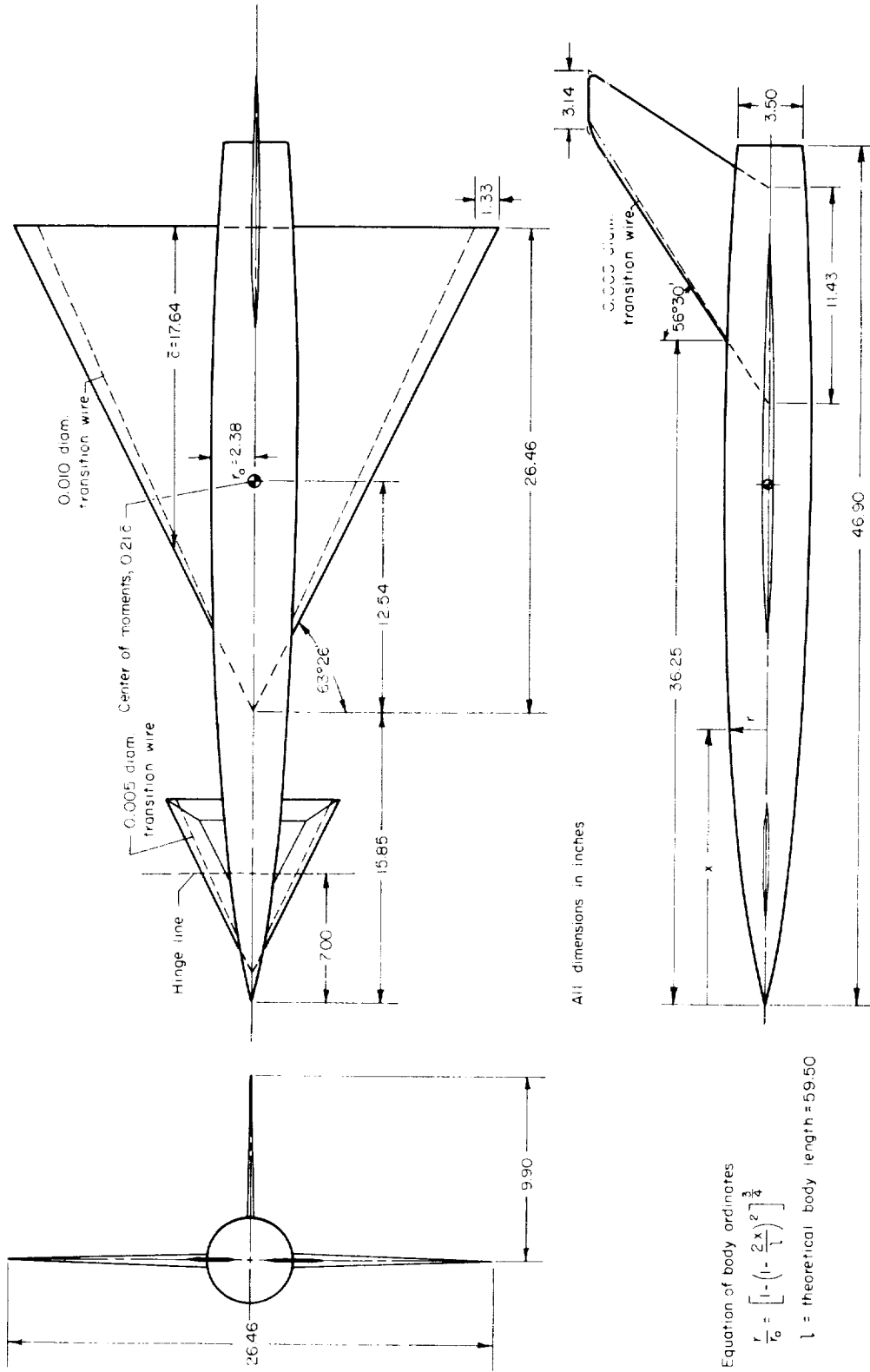
Equation of body ordinates

$$\frac{r}{r_0}=\left[1-\left(1-\left(\frac{2x}{l}\right)^2\right)\right]^{\frac{3}{4}}$$

l = theoretical body length = 59.50

(e) Dimensional sketch of single-tail model of references 2 and 3.

Figure 1.- Concluded.

A508
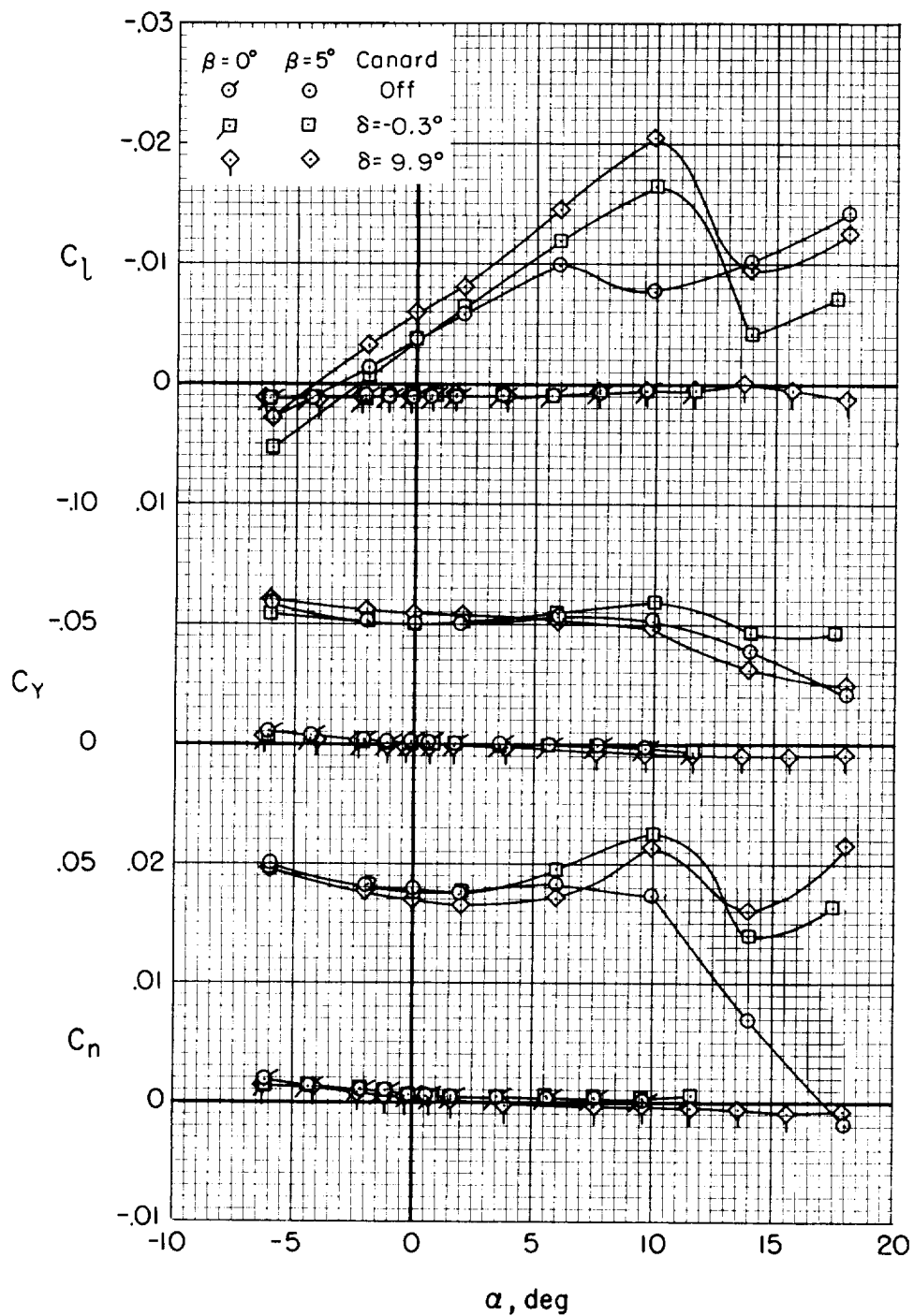
(a) M = 0.70

Figure 2.- Rolling-moment, side-force, and yawing-moment characteristics of the model for 0° and 5° sideslip.

16
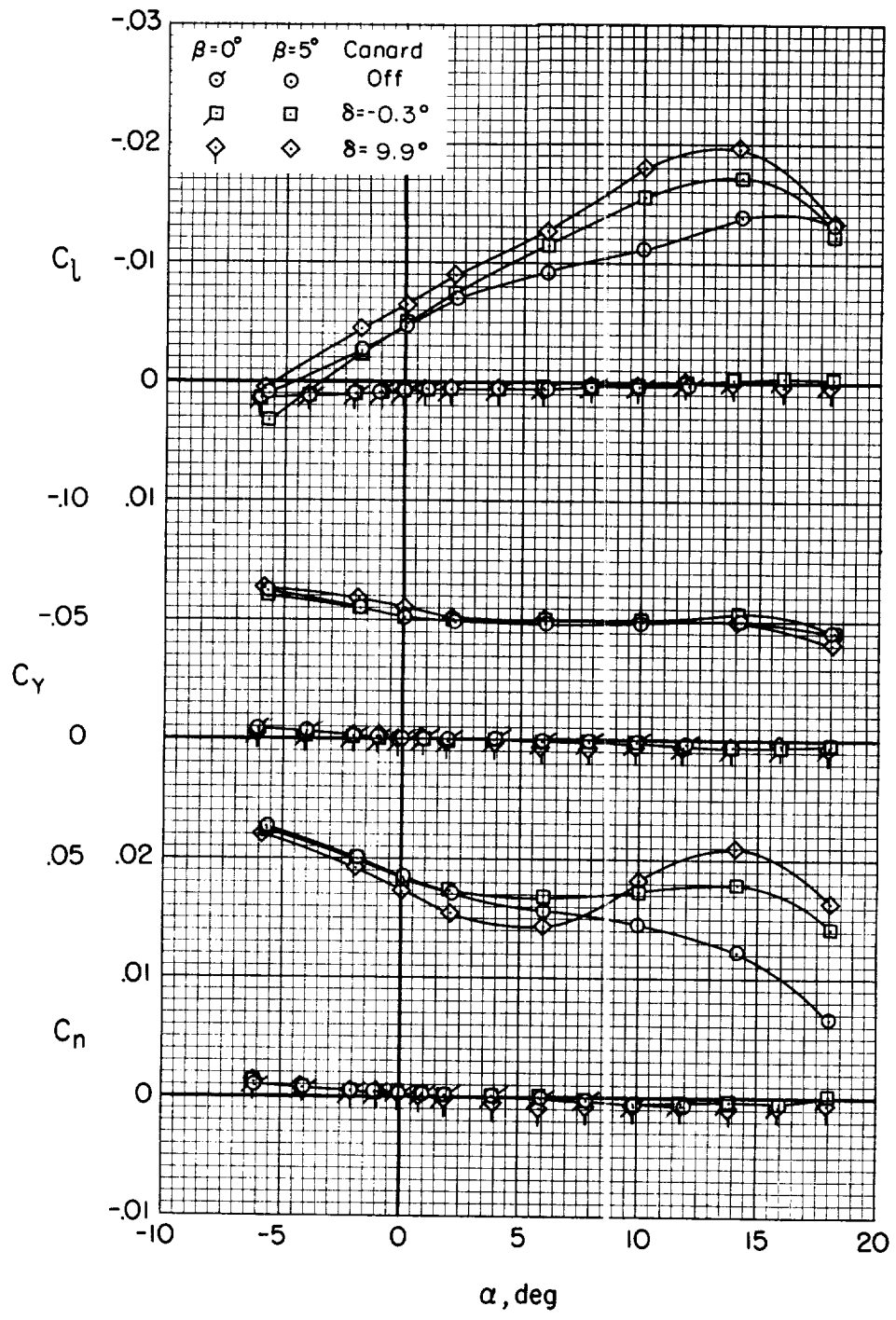
(b) M = 1.30

Figure 2.- Continued.

A
5
0
8
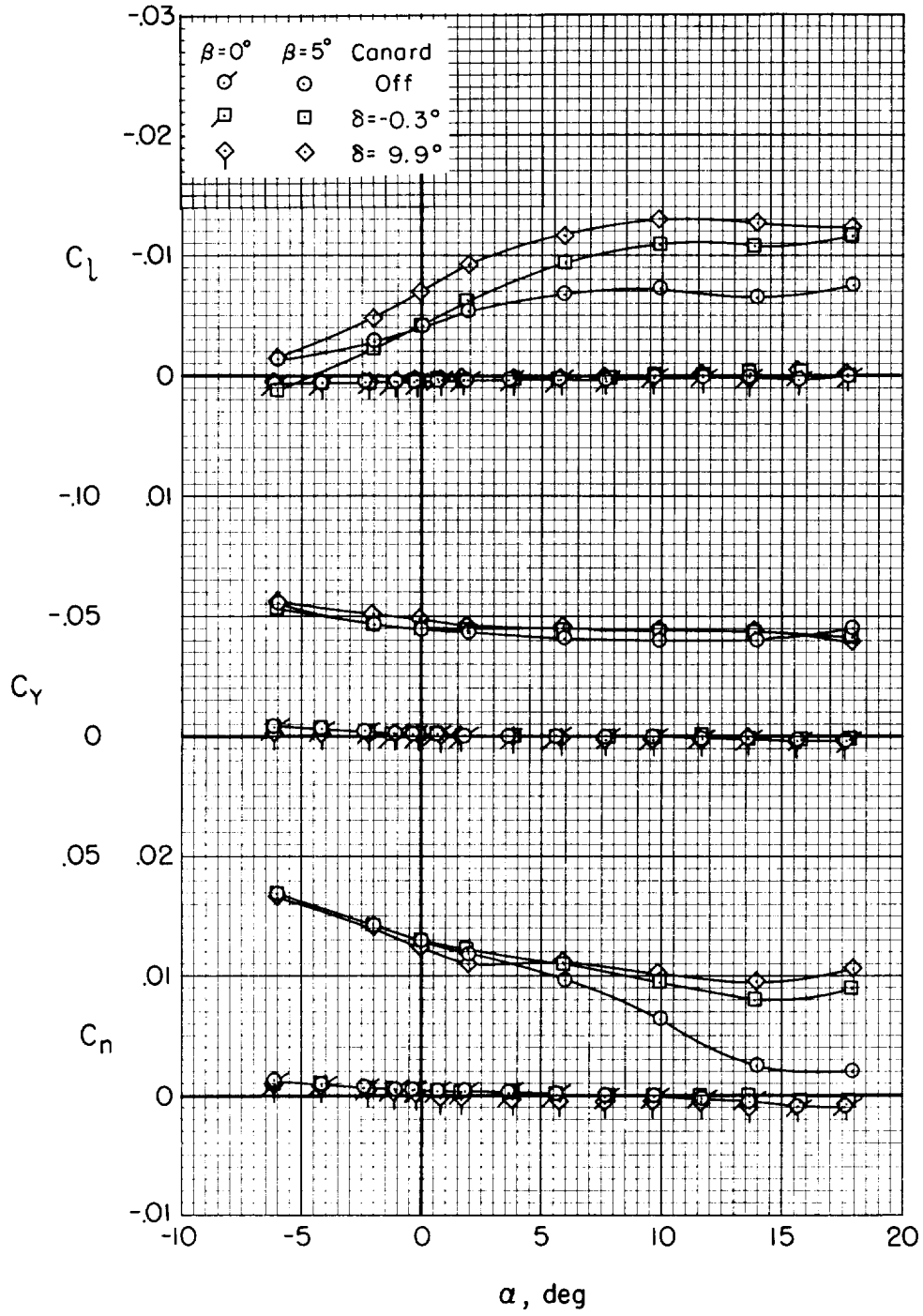
(c) M = 1.70

Figure 2.- Continued.
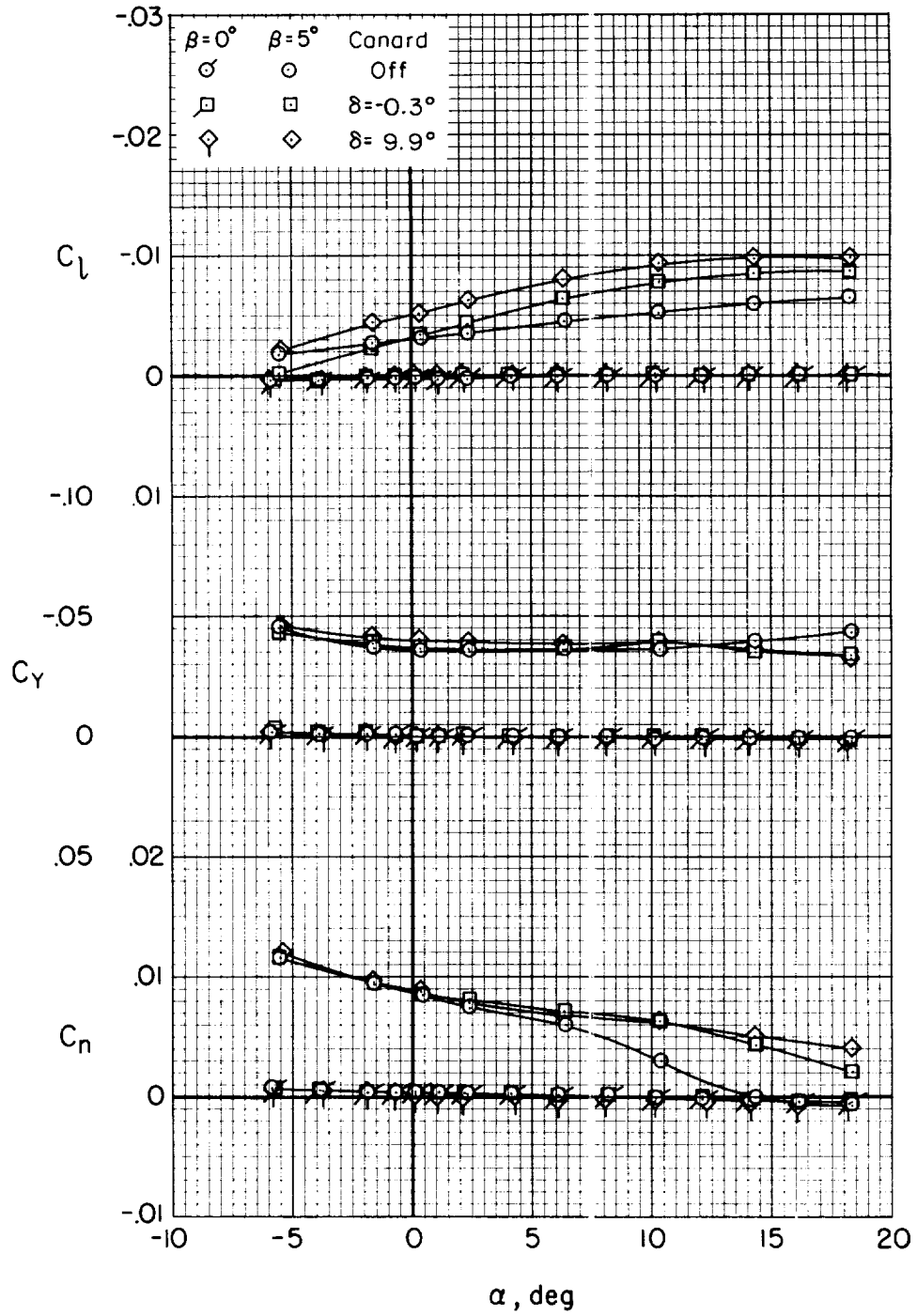
(d) M = 2.22

Figure 2.- Concluded.
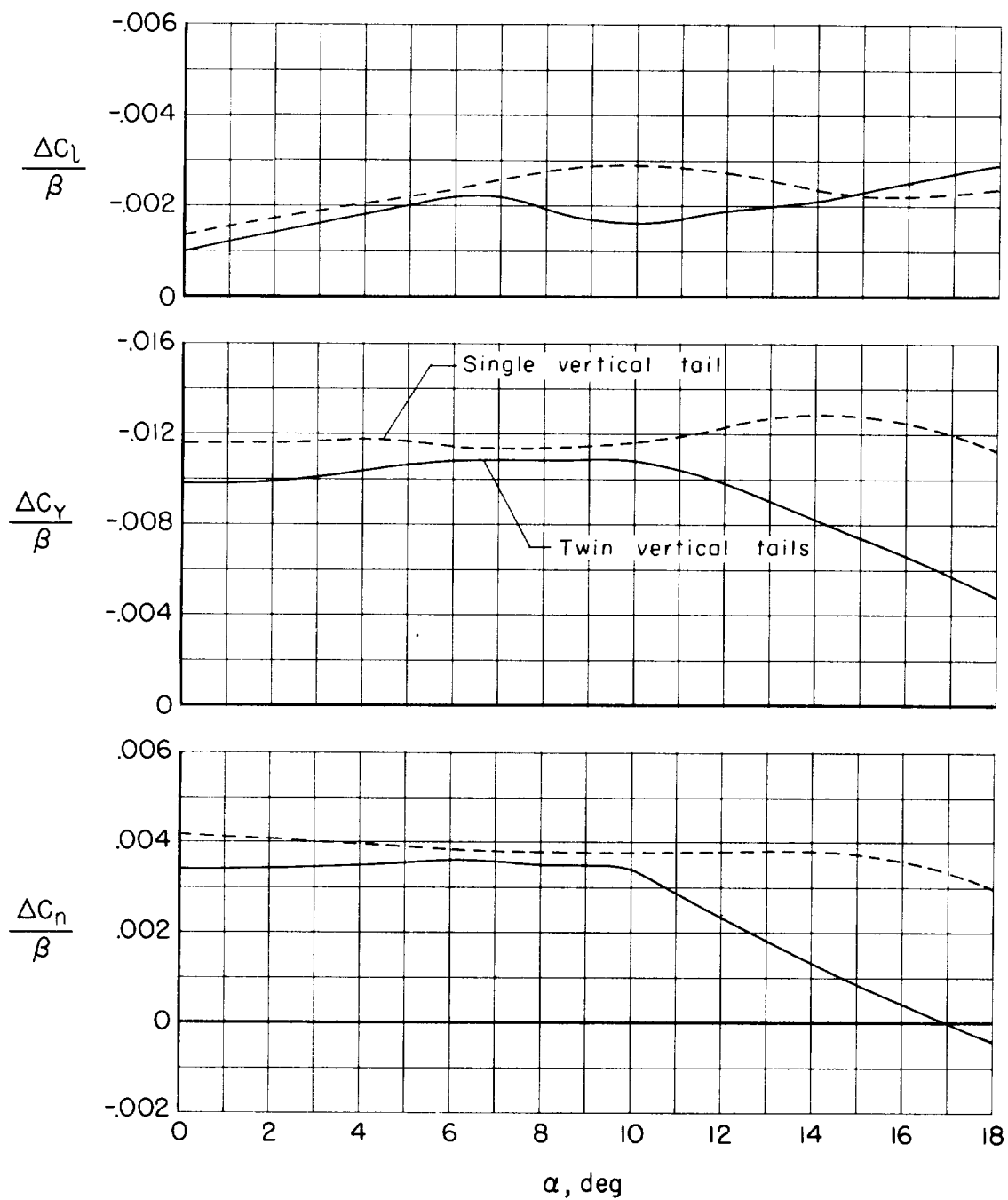
(a) M = 0.70

Figure 3.- Comparisons of the lateral and directional aerodynamic
characteristics of the twin-tail model without canard with those
of the single-tail model of reference 3.
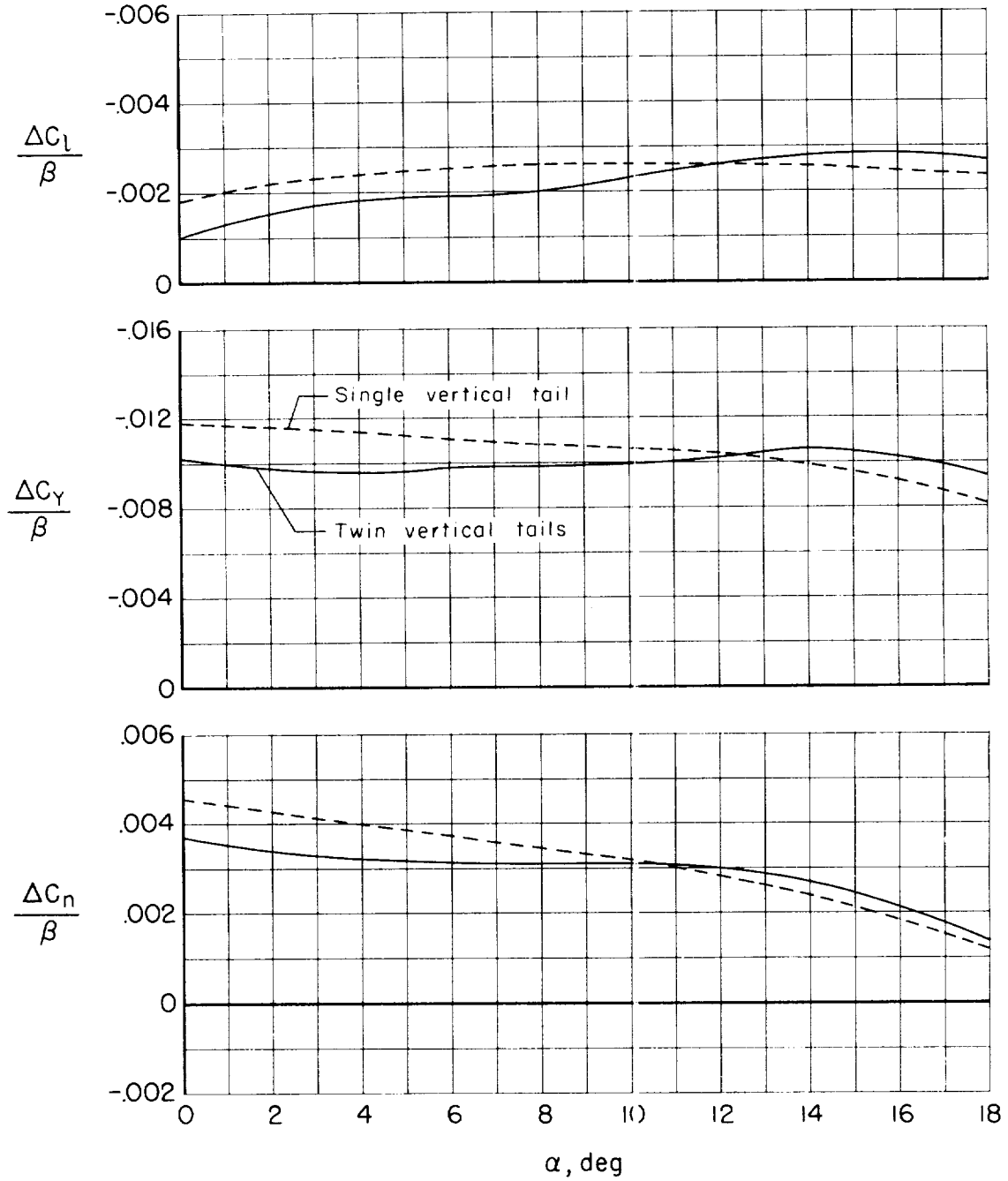
(b) M = 1.30

Figure 3.- Continued.
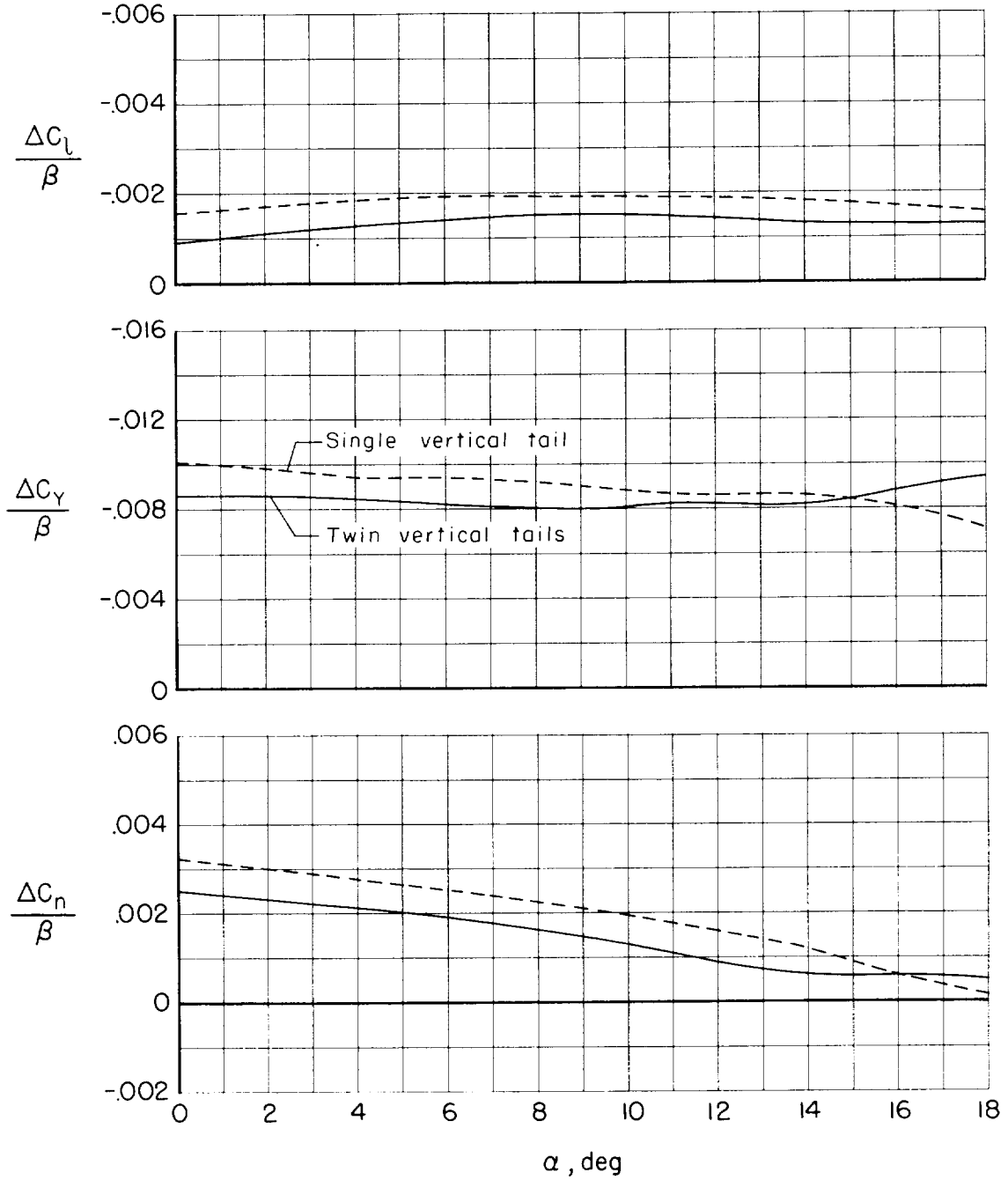
(c) M = 1.70

Figure 3.- Continued.
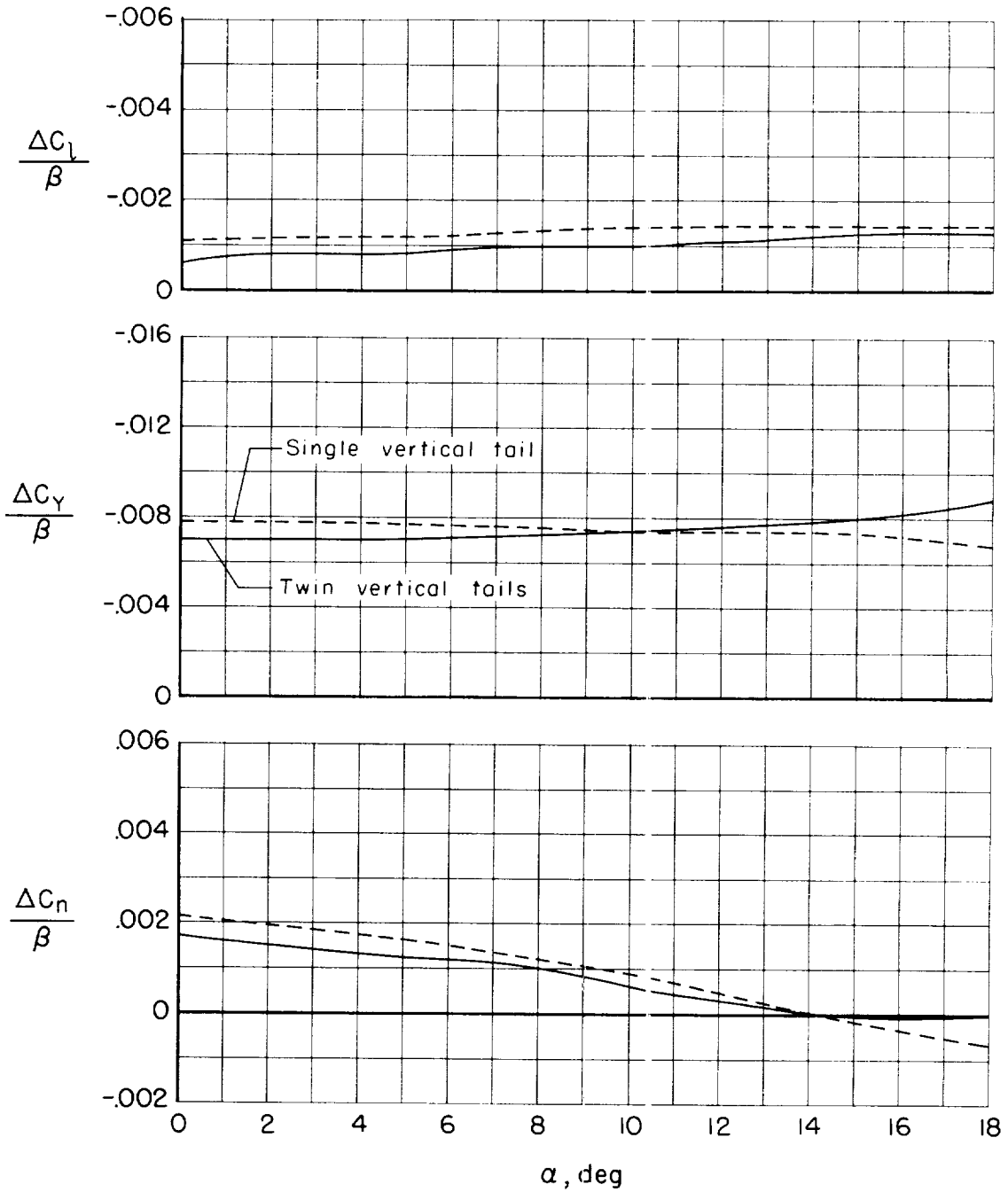
(d) M = 2.22

Figure 3.- Concluded.

A
5
0
8
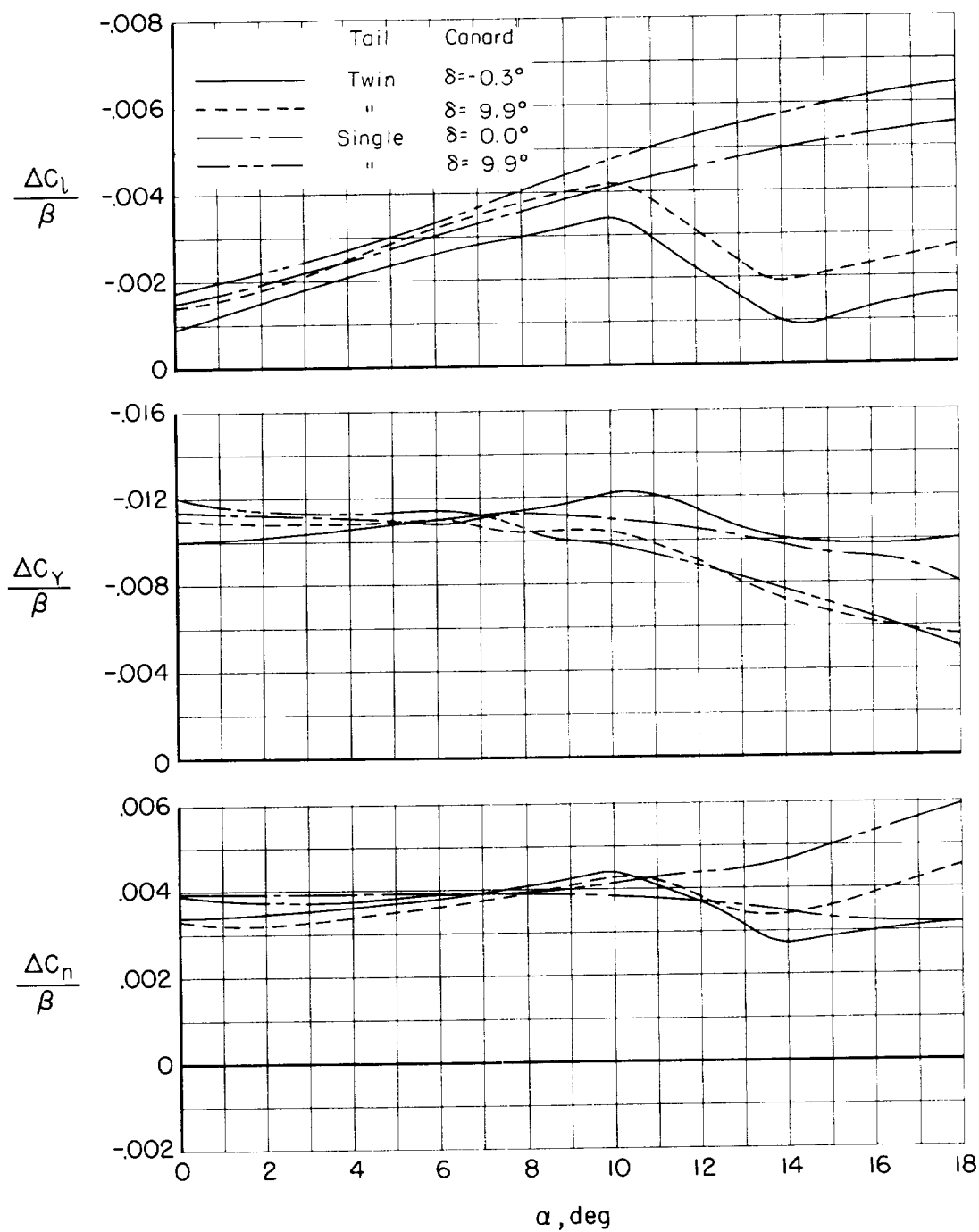
(a) M = 0.70

Figure 4.- Comparisons of the lateral and directional aerodynamic
characteristics of the twin-tail model with canard with those
of the single-tail model of reference 3.
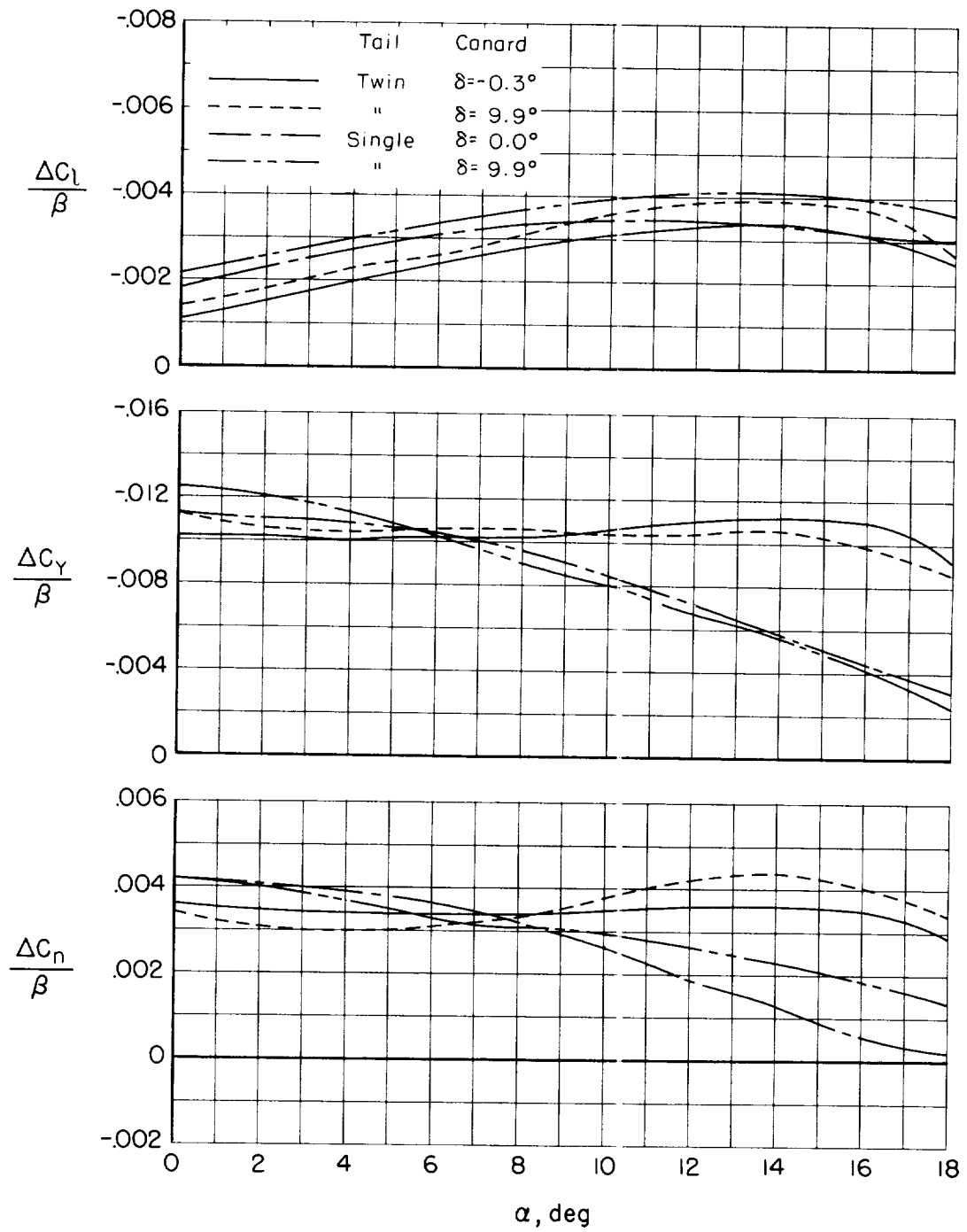
(b) M = 1.30

Figure 4.- Continued.
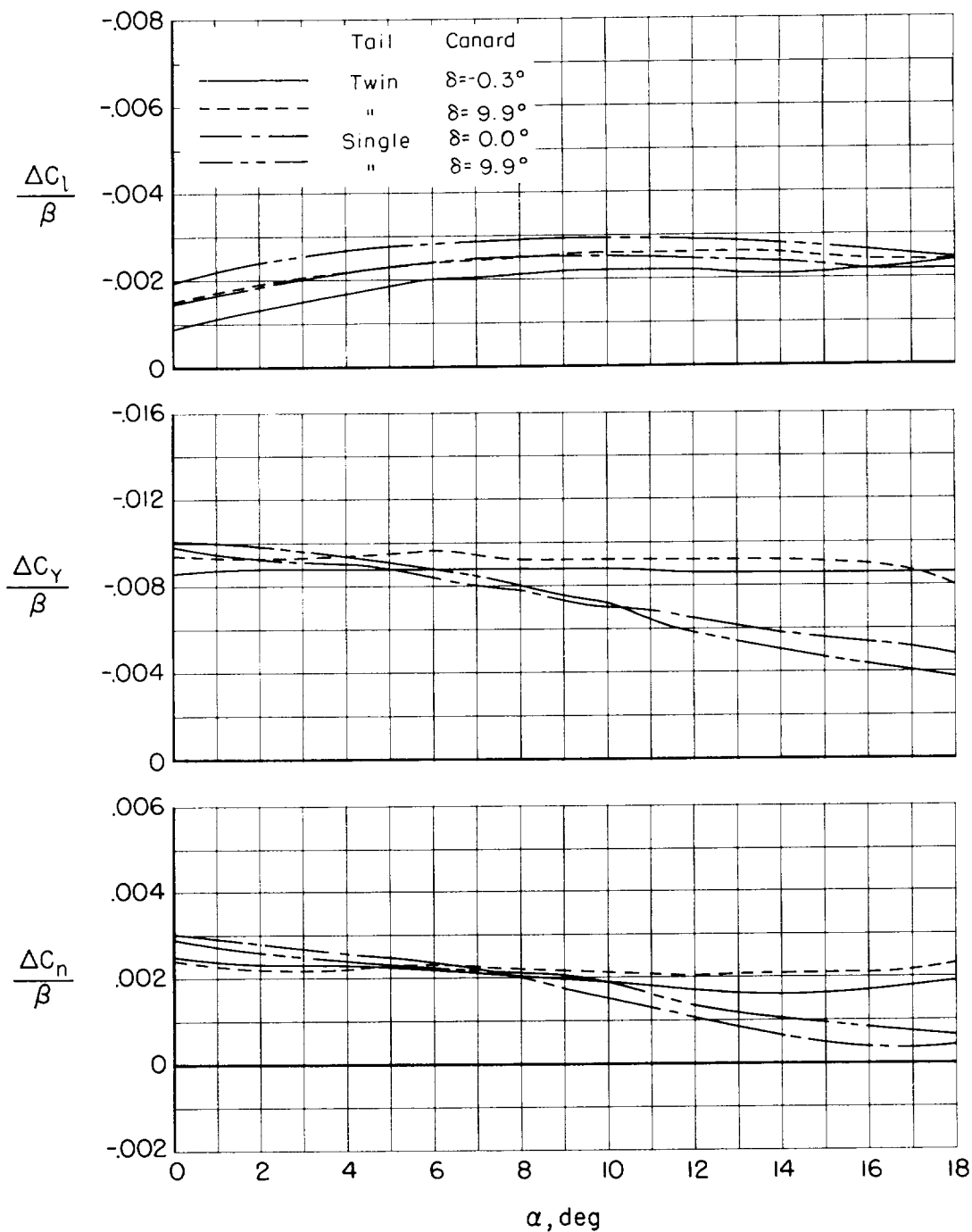
(c) M = 1.70

Figure 4.- Continued.
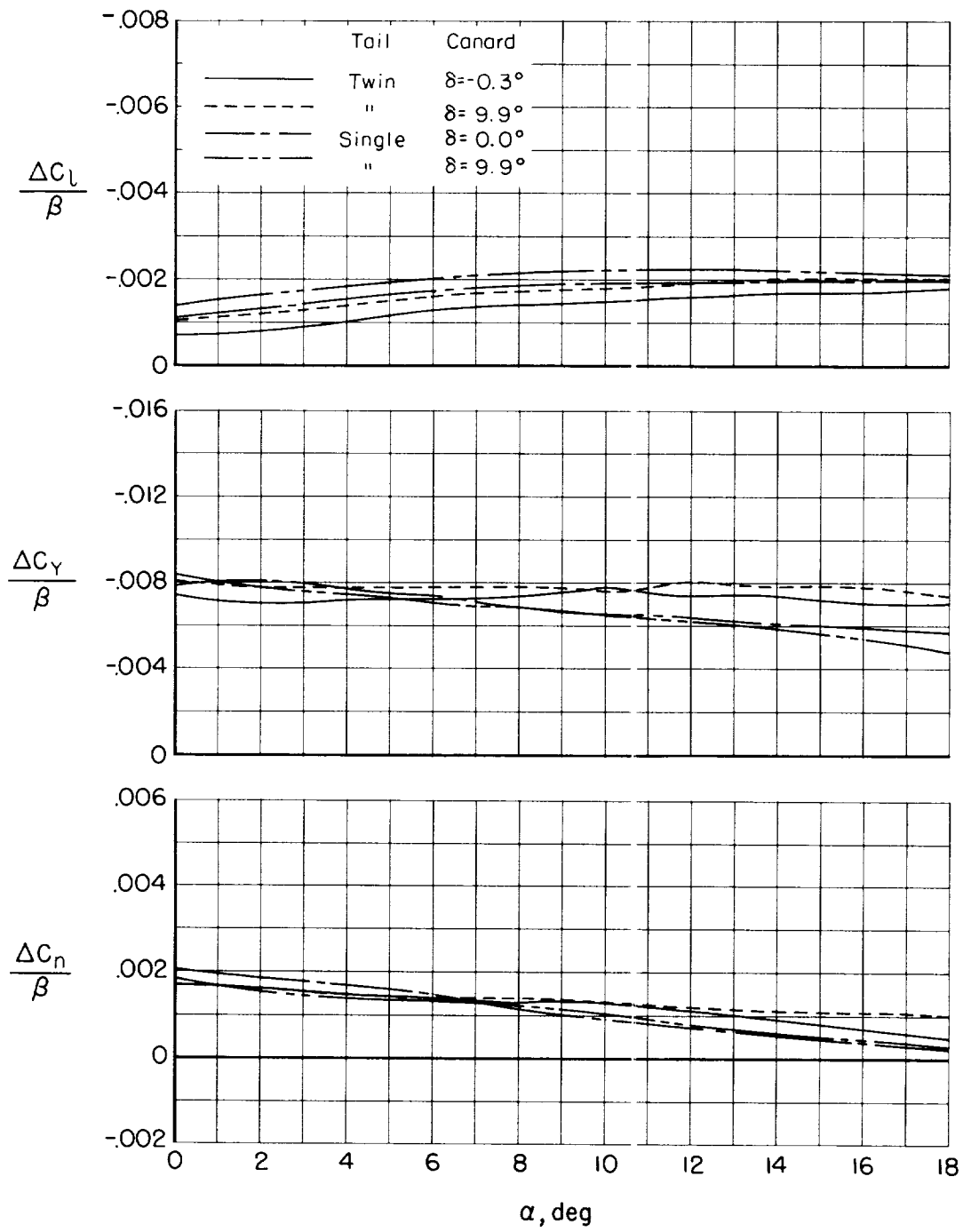
(d) M = 2.22

Figure 4.- Concluded.
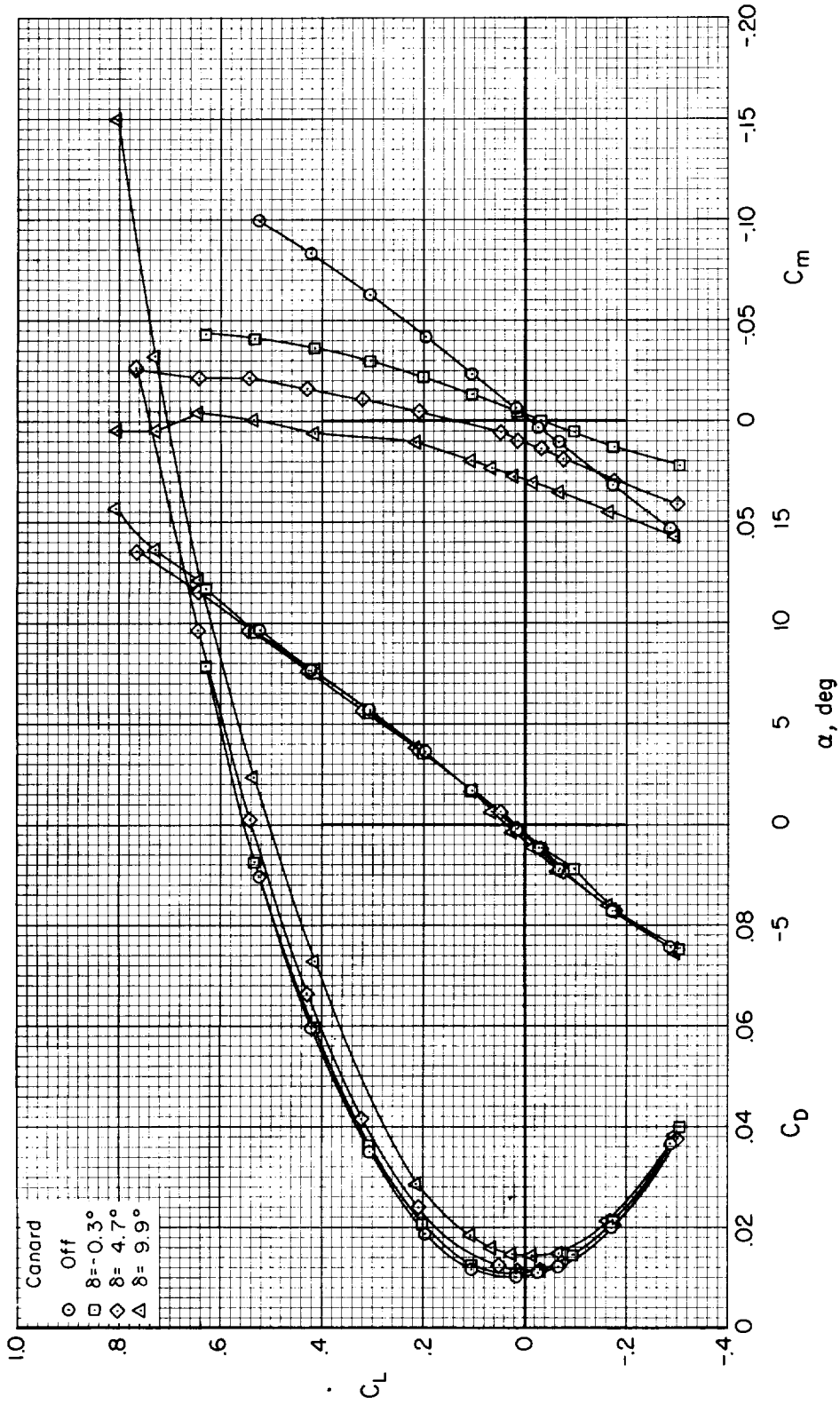
(a) M = 0.70

Figure 5.- Lift, drag, and pitching-moment characteristics of the model for 0° sidesⅬip.
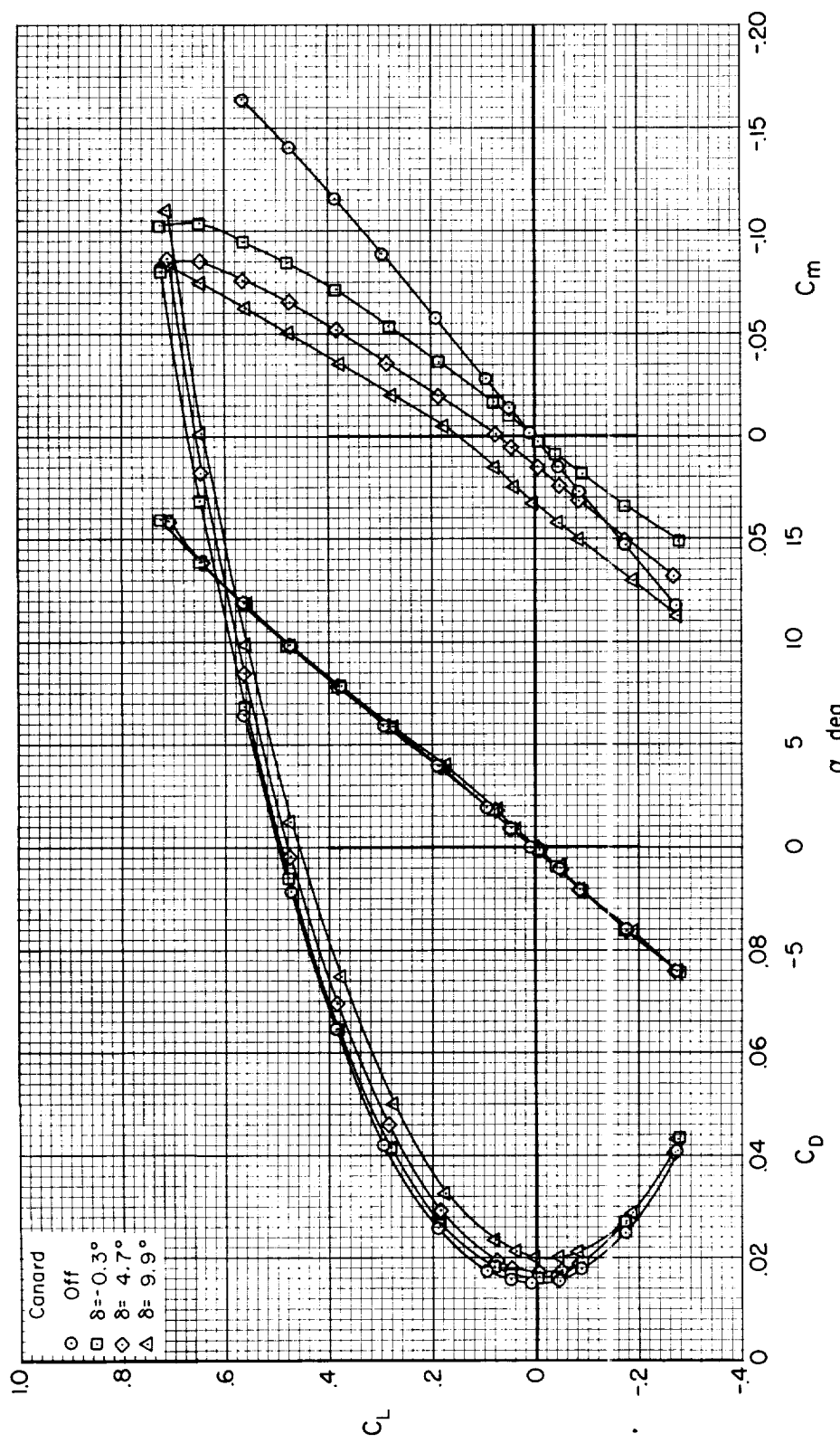
(b) M = 1.30

Figure 5.- Continued.
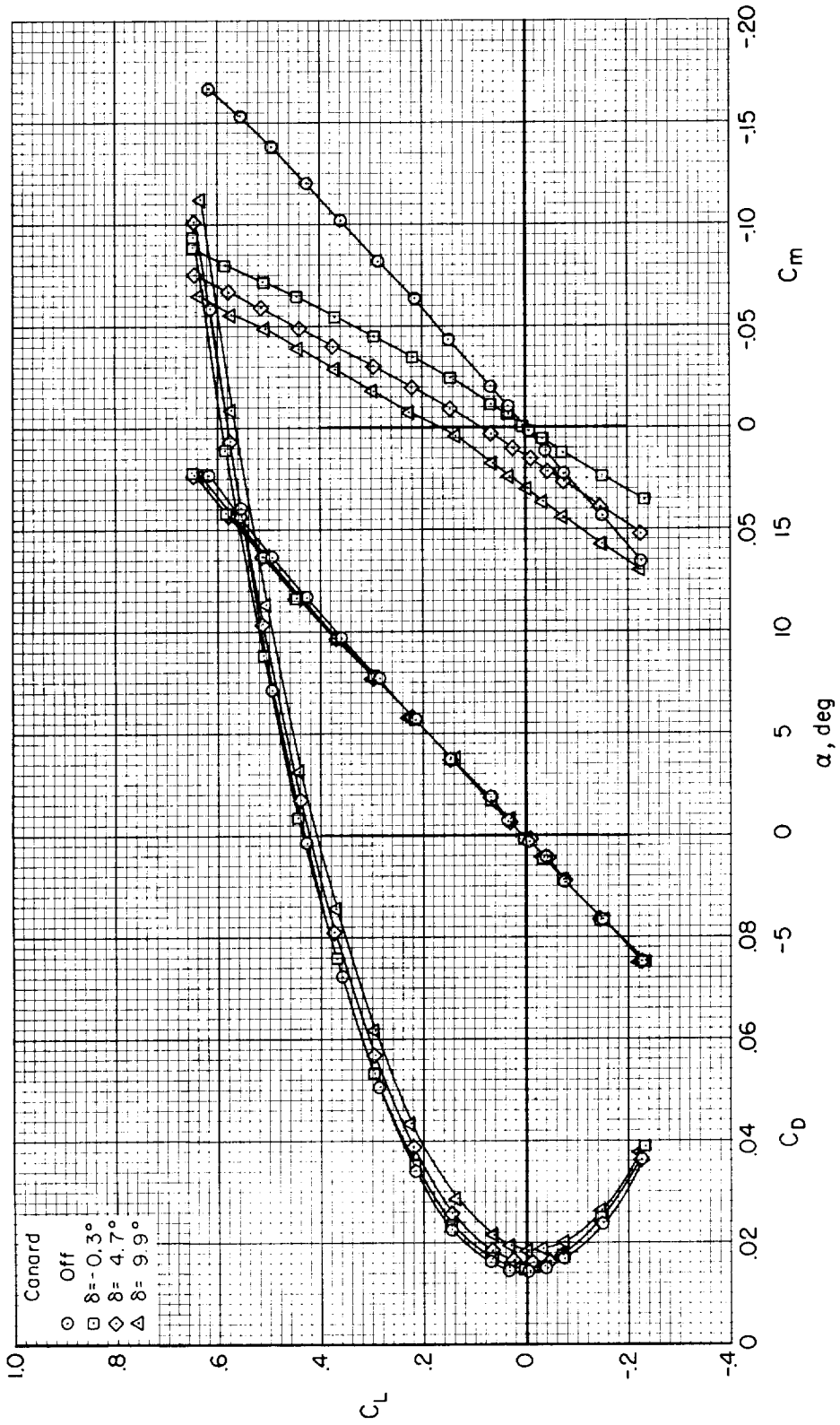
(c) M = 1.70

Figure 5.- Continued.
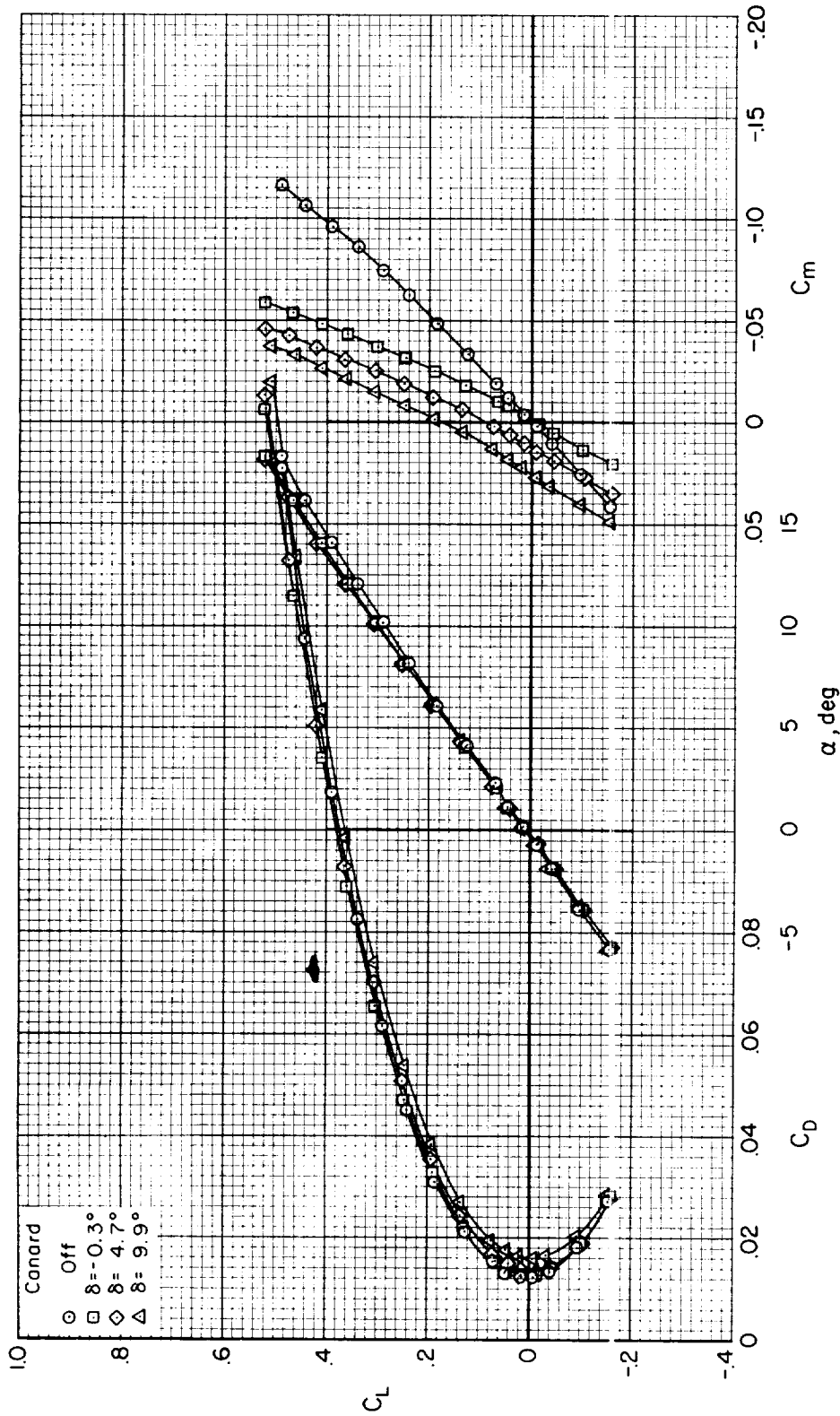
(d) $M = 2.22$

Figure 5.- Concluded.

A 5 0 8
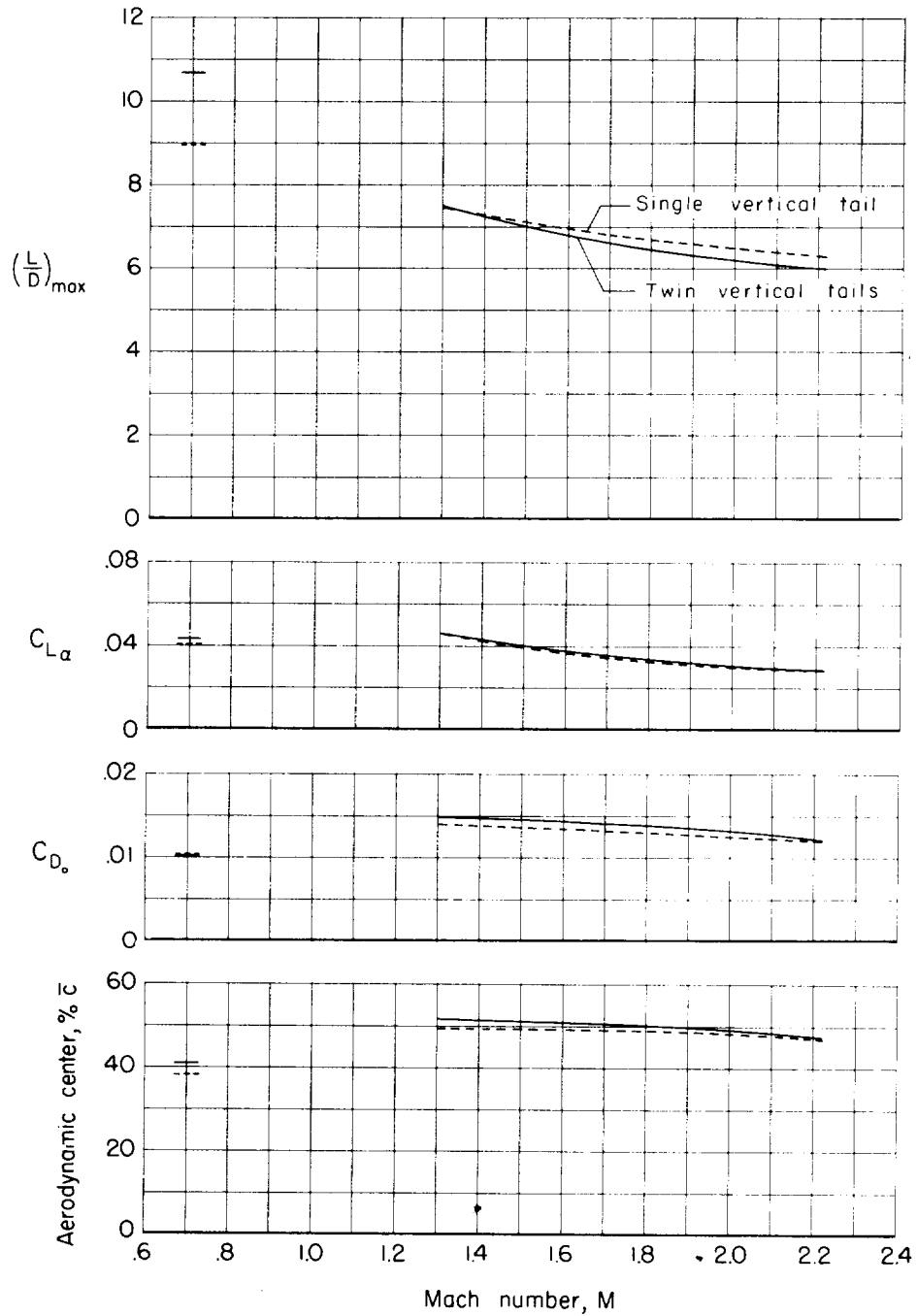
(a) Canard off.

Figure 6.- Comparisons of the longitudinal aerodynamic characteristics of the twin-tail model with those of the single-tail model of reference 2; $\beta = 0^{\circ}$.
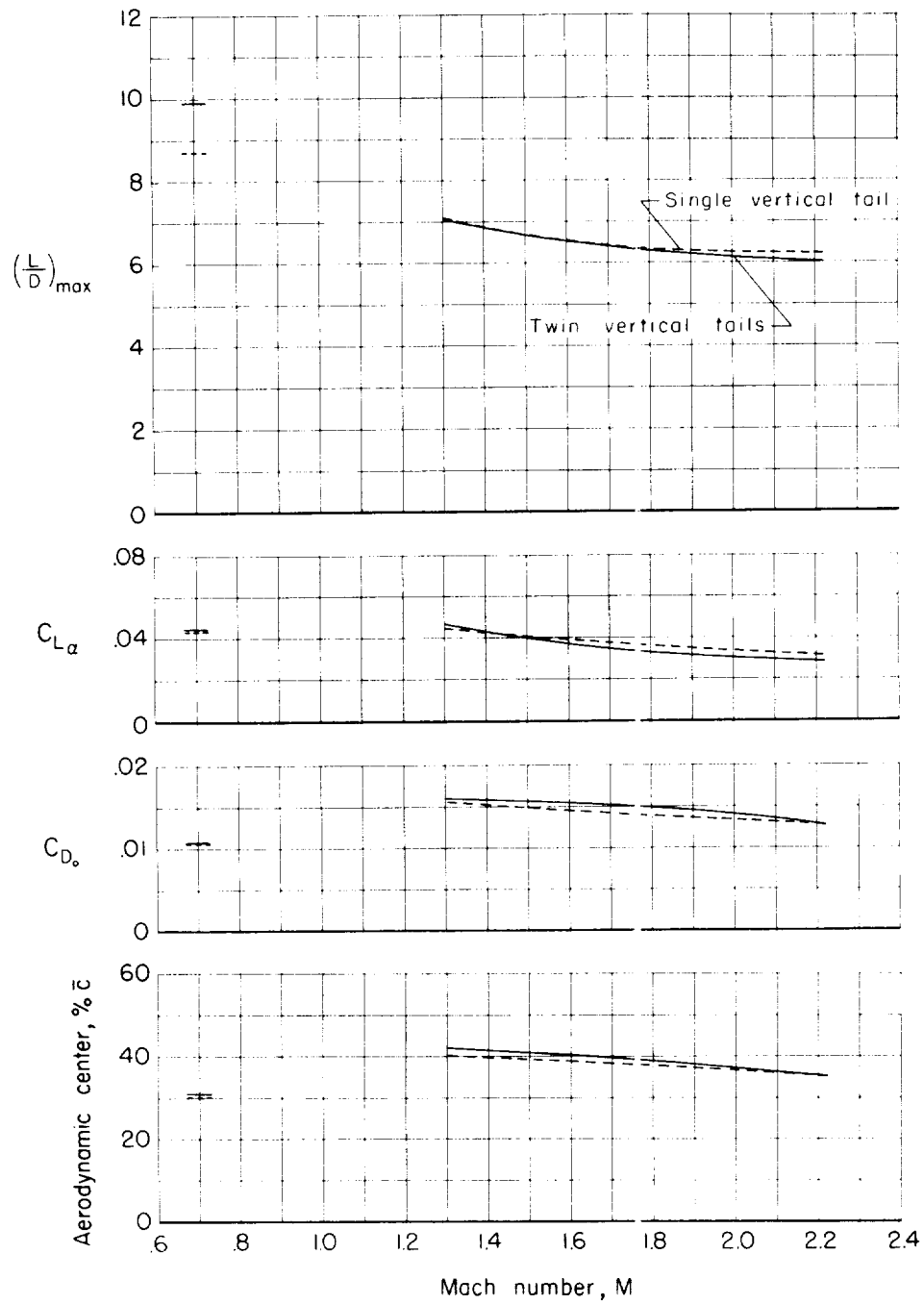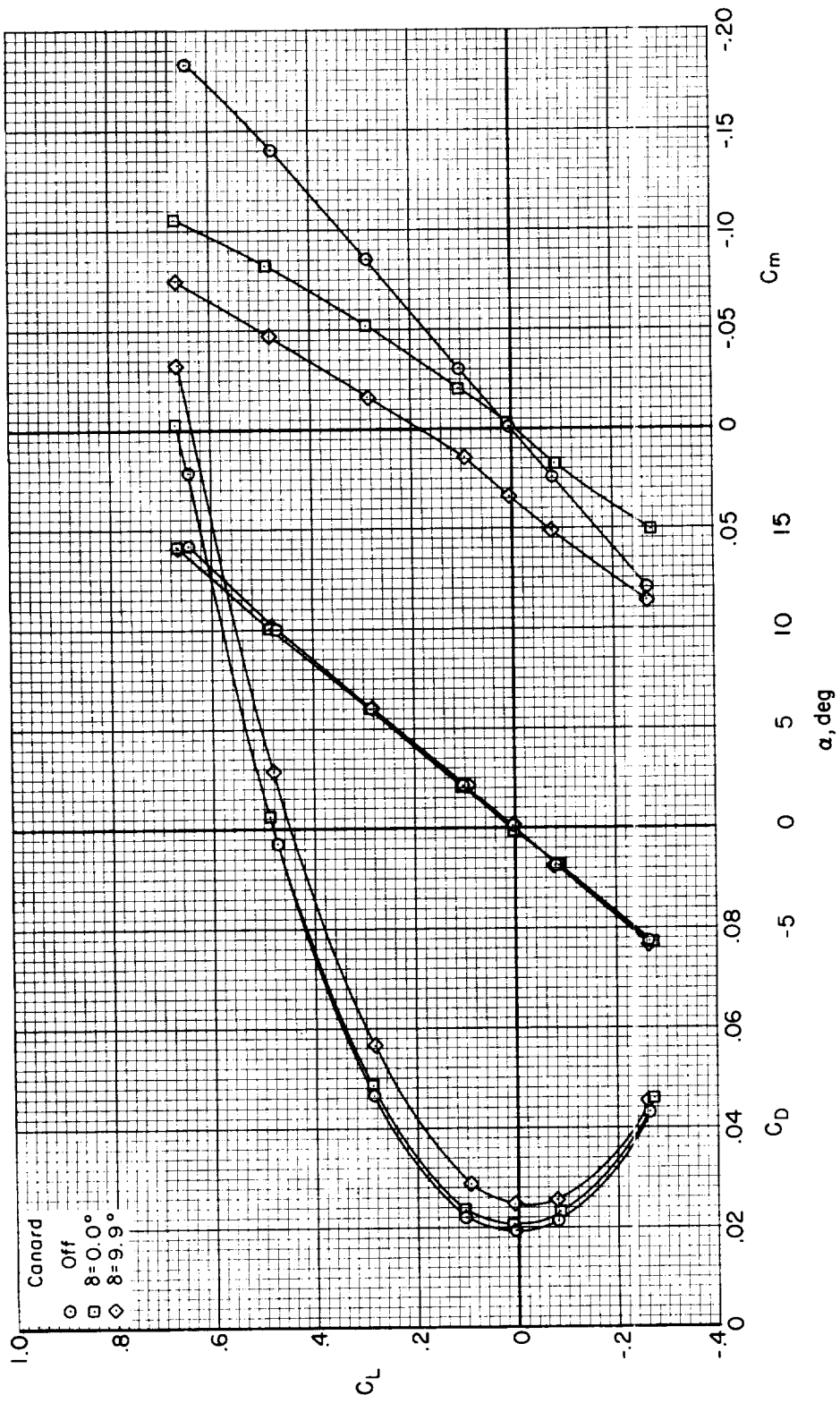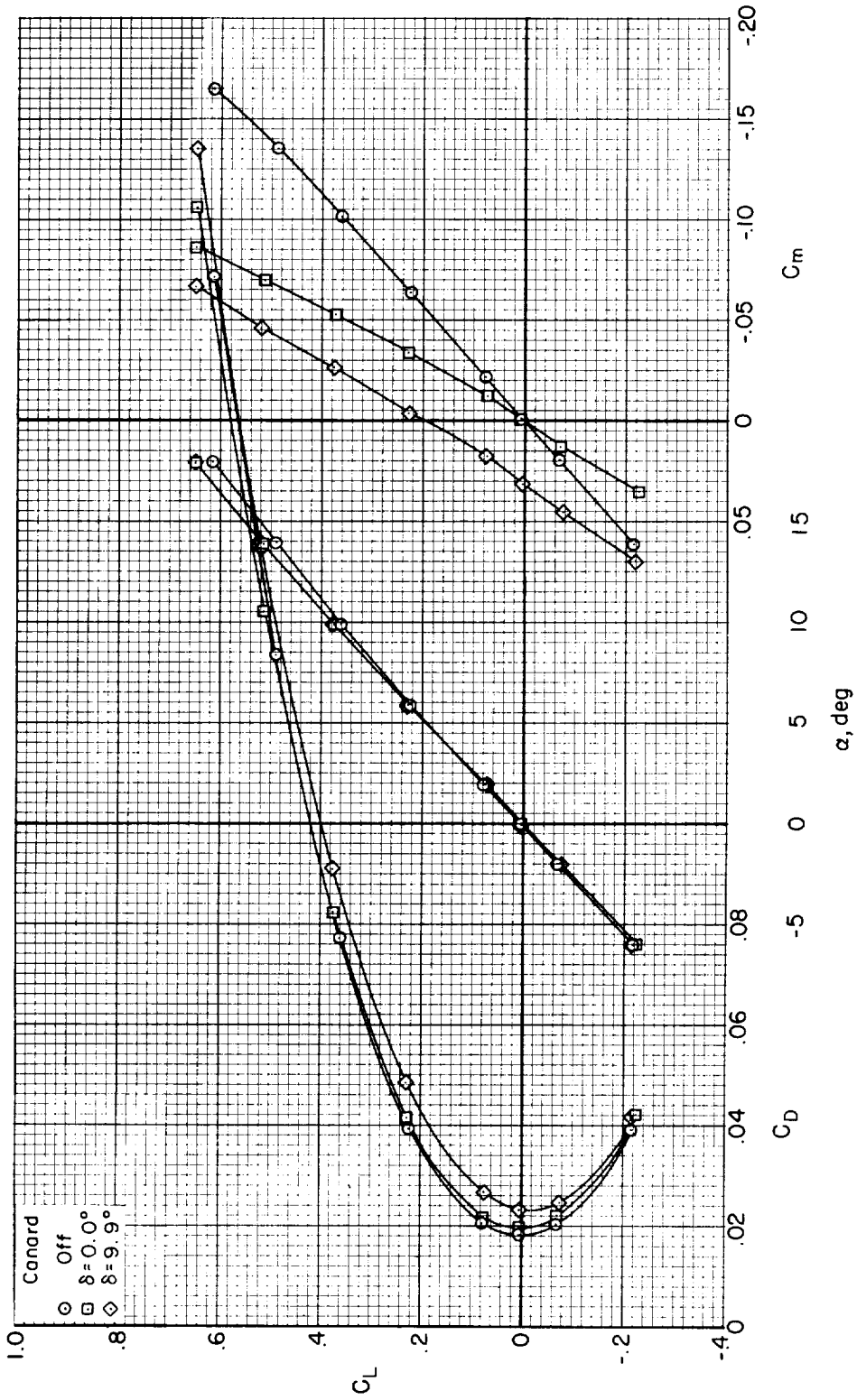
(b) Canard on.

Figure 6.- Concluded.
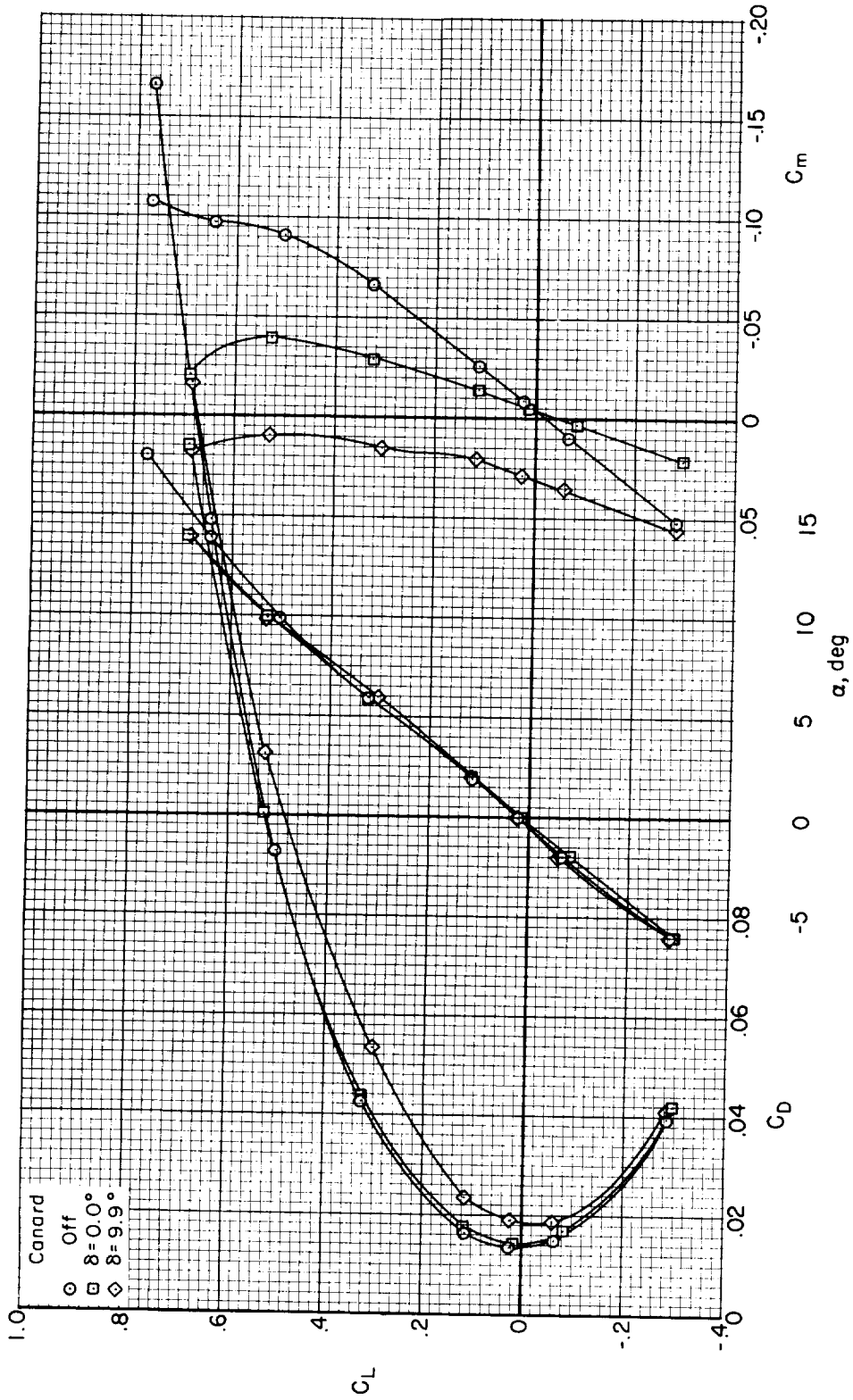
(a) M = 0.70

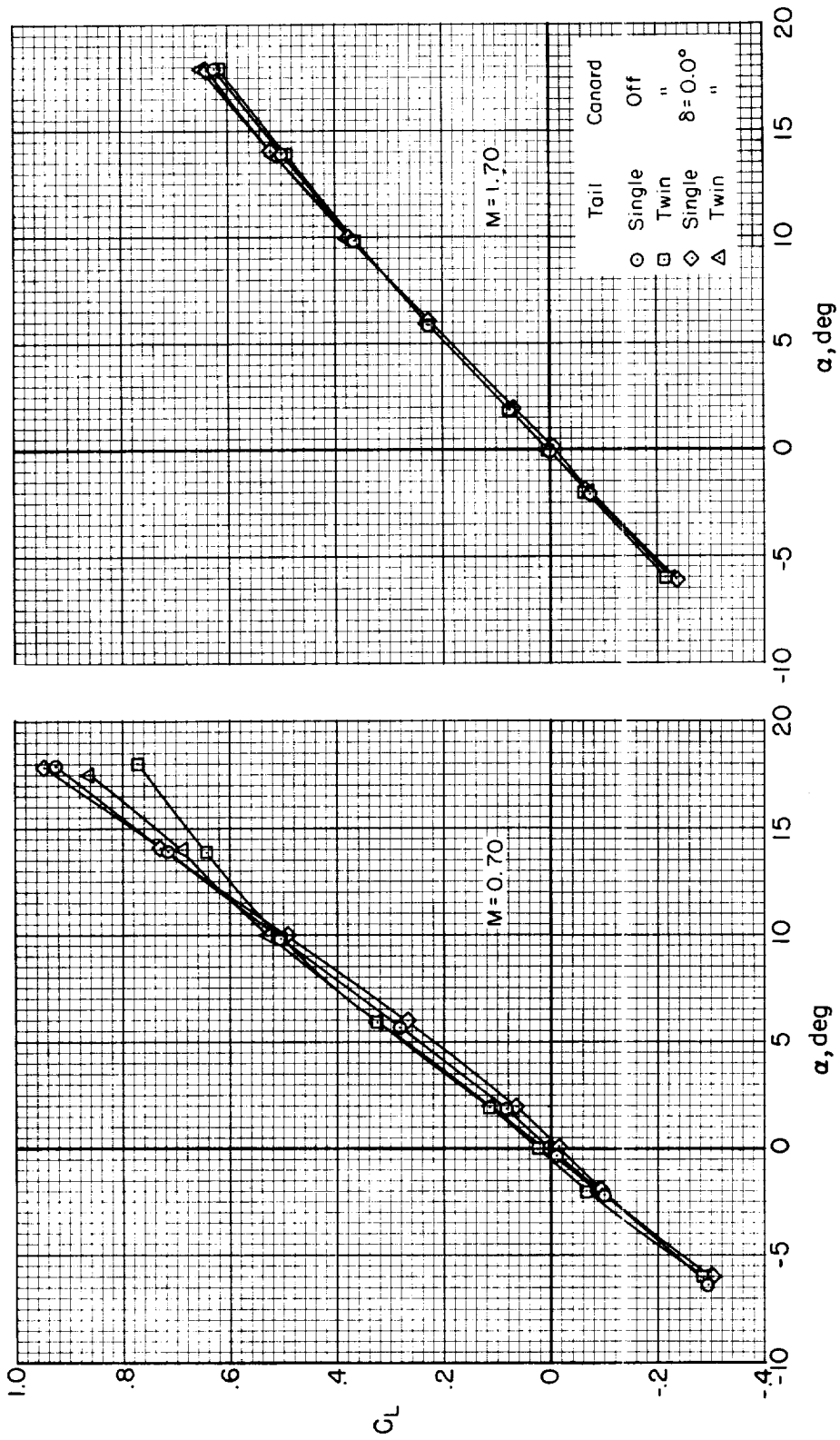Figure 7.- Lift, drag, and pitching-moment characteristics for 5° sideslip.

(b) M = 1.30

Figure 7.- Continued.

(c) M = 1.70

Figure 7.- Continued.

(b) Lift characteristics.

Figure 8.- Concluded.